Pattern formation in reaction-diffusion systems – an explicit approach

Arjen Doelman
Mathematisch Instituut, Leiden University,
P.O. Box 9512, 2300 RA Leiden, the Netherlands,
doelman@math.leidenuniv.nl

May 25, 2018

Abstract

Pattern formation is the sub-area of complexity science in which the dynamics of nonlinear spatial processes is studied. Reaction-diffusion systems appear as relevant models for such processes and are at the core of the mathematical analysis of pattern formation. This review presents an introduction to the basic mathematical 'tools' by which an understanding of complex pattern dynamics can be built. For simplicity, it focuses on 2-component reaction-diffusion systems in one spatial dimension. In this setting the techniques by which pattern formation can be studied – both 'near onset' as well as 'far from equilibrium' – can be presented in such a way that an explicit study of a given model can be set up. Moreover, the text provides furthers steps by which more complex patterns in more complex systems than considered here may be understood.

1 Introduction

The study of the formation, evolution and dynamics of spatial patterns, and especially of reaction-diffusion patterns, takes place at the intersection of classical disciplines as biology, chemistry, mathematics and physics. Multi-component systems of reaction-diffusion equations serve as relevant – often simplified – models for fundamental mechanisms such as the distribution and transport of action potential over nerve axons or along a beating heart, or the response of an ecosystem to changing climatological circumstances – see the textbooks [46, 49, 53, 57] for a multitude of explicit biological, chemical and ecological model systems. In mathematics, reaction-diffusion systems are considered as the most simple evolutionary processes that exhibit complex spatial patterns. In fact, even models with only 2 components – or 'species' – generate strikingly rich spatio-temporal dynamics – see Fig. 1. Through this combination of direct relevance and (relative) mathematical simplicity, reaction-diffusion systems play a crucial role in the (sub)area of complexity theory within which a fundamental understanding of the formation and dynamics of spatio-temporal patterns is developed.

Although there certainly are a number of introductory texts on reaction-diffusion equations in the mathematical literature – see for instance [33, 41, 78, 82, 92, 95] – there still is a gap between the phenomenology of reaction-diffusion patterns studied in the biology/chemistry/physics literature and the availability of mathematical 'tools' by which the first steps towards building a fundamental understanding of the pattern dynamics of a given *explicit* reaction-diffusion model can be taken. This review aims at providing an introduction to some of the most basic mathematical 'tools' – in the most simplified setting – in such a way that these tools can indeed be applied to a given explicit reaction-diffusion model.

In its most general form, an N-component reaction-diffusion system for $\mathbf{U} = (U_1, ..., U_N) \in \mathbb{R}^N$ is given by,

$$\mathbf{U}_t = D\Delta\mathbf{U} + \mathbf{F}(\mathbf{U};\mu), \tag{1.1}$$

in which $\mathbf{U}(x,t)$ depends on $(x,t) \in \Omega \times \mathbb{R}^+$ with (spatial) domain $\Omega \subset \mathbb{R}^n$ (typically $n = 1, 2, 3$), D is a diffusion matrix (i.e. a diagonal $N \times N$ matrix with strictly positive entries), Δ is the Laplace/diffusion operator, and the vector field $\mathbf{F}(\mathbf{U};\mu) : \mathbb{R}^N \to \mathbb{R}^N$ represents the (nonlinear) reaction terms; moreover, (1.1) depends on (a number of) parameters $\mu \in \mathbb{R}^m$ – Remark 1.1(Throughout the text, subscripts in t, τ, x and ξ denote differentiation.) To keep the presentation as transparent as possible – the explicit study

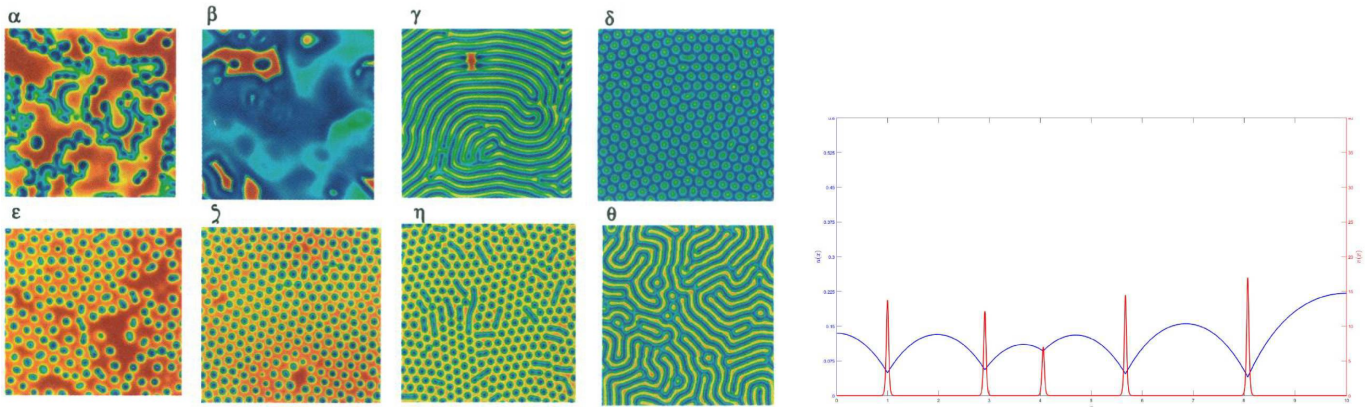

Figure 1: Numerical simulations of pattern formation in the Gray-Scott model [51, 63], i.e. $G(U,V) = A(1-U) - UV^2$, $H(U,V) = -BV + UV^2$ in (1.2). (a) $\alpha - \theta$ from [63]: snapshots of dynamically evolving patterns in 2 (space) dimensions for various choices of parameters A and B (with $d \equiv 0.5$) – colors indicate the value of the U-component; (b) snapshot of an evolving 1-dimensional singularly perturbed multi-pulse pattern (with $d = 0.01$); 'slow' U-component in blue, 'fast' V in red.

of patterns is quite a technical endeavor – we restrict ourselves here mainly to the simplest case that still generates rich pattern dynamics: 2-component systems – i.e. $N = 2$ in (1.1) – defined on the *unbounded* 1-dimension domain $\mathbb{R}$ – i.e. $\Omega = \mathbb{R}^1$ – see Fig. 1(b). Note that our choice for Ω eliminates the effect boundary conditions may have on the patterns generated by a model. Thus, we write (1.1) as,

$$\left\{ \begin{array}{lllll} U_t & = & U_{xx} & + & G(U,V;\mu), \\ V_t & = & dV_{xx} & + & H(U,V;\mu), \end{array} \right. \tag{1.2}$$

in which $\mathbf{U}$ is now written as (U,V) and $\mathbf{F}(\mathbf{U};\mu)$ as $(G(U,V;\mu), H(U,V;\mu))$; by rescaling x, D has diagonal elements 1 and d, the ratio of the diffusion coefficients of components U and V.

A mathematical study of patterns exhibited by system (1.2) 'must' start with determining the 'trivial patterns' $(U(x,t), V(x,t)) \equiv (\bar{U}, \bar{V}) = (\bar{U}(\mu), \bar{V}(\mu))$ of (1.2) – the solutions of the algebraic system $G(\bar{U}, \bar{V}; \mu) = H(\bar{U}, \bar{V}; \mu) = 0$ which are constant, 'homogeneous', in space and time – immediately followed by a spectral stability analysis. This is also how we set up this text: in section 2.1 we present the linear algebra that determines the stability of $(\bar{U}, \bar{V})$. We focus on the mechanisms by which $(\bar{U}, \bar{V})$ may be destabilized: this determines the *onset of pattern formation*. Since it is the first step towards the formation of *Turing patterns* [57, 83], the linear analysis of section 2.1 is commonly known – also to many non-mathematicians. However, in sections 2.2-2.4 we also present the necessary – but often neglected – *weakly nonlinear Ginzburg-Landau analysis* by which the possible appearance of (small amplitude) Turing patterns can be established. We show how to determine whether the linear Turing destabilization corresponds to *a sub- or a supercritical bifurcation* and that only the latter case generates Turing patterns.

The trivial background states $(\bar{U}, \bar{V})$ also plays a crucial role in the second main part of this text, section 4 on localized solutions 'far from equilibrium'. The approach is similar to that of section 2, in the sense that we present in detail some of the basic insights on the existence and stability of stationary symmetric 'pulse' solutions of reaction-diffusion system (1.2). Like the Turing/Ginzburg-Landau analysis of section 2, these results are scattered throughout the literature and not readily available to non-specialists. As main outcome of this section, we present two explicit results on the existence and stability of pulses in *singularly perturbed* systems – indicating how similar results could be obtained for other types of far from equilibrium patterns.

Section 3 introduces a concept that is much less classical in the literature on reaction-diffusion equations: the Busse balloon – which originates from fluid mechanics [6]. It provides a natural 'bridge' between the near onset and far from equilibrium settings of sections 2 and 4. Finally, the text concludes with a section on more complex patterns – such as interacting localized structures – in more extended systems – such as system (1.1) with $N, n \geq 2$. This section builds on the approaches and tools developed in sections 2-4 and intends to provide further steps towards understanding the foundations of the complexity of evolving spatial processes.

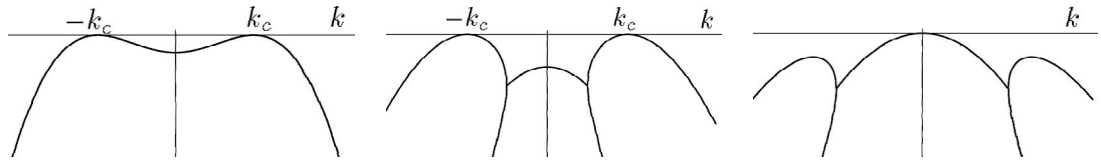

Figure 2: Three critical eigenvalue curves. (a,b): The real parts of the solutions $\lambda_{1,2}(k)$ of (2.2) for a Turing destabilization – i.e. $k_c \neq 0$ – with $\lambda_{1,2}(k) \in \mathbb{R}$ for all $k \in \mathbb{R}$ in (a), and parameter combinations such that $\lambda_{1,2}(k) \notin \mathbb{R}$ for certain k in (b). (c): A $k_c = 0$-case that corresponds to a Hopf bifurcation in the reaction ODE (2.7).

Remark 1.1 As usual, we assume that parameters $\mu \in \mathbb{R}^m$ are constants, i.e. that they do not vary in time and/or space. In realistic settings, this is a *huge* oversimplification – in biology and especially ecology parameters such as 'yearly rainfall' vary significantly, both time and in space [53, 76, 77]. The mathematical analysis of the impact of 'heterogeneous parameters' is at its infancy – see [27] and the references therein.

2 The onset of pattern formation: the Turing bifurcation

2.1 Spectral analysis: the Turing destabilization

Since we consider (1.2) on the unbounded domain $\mathbb{R}$, and since we assume that there are no terms in (1.2) that depend explicitly on t or x (Remark 1.1), the spectral – or linearized – stability of trivial pattern $(\bar{U}, \bar{V})$ against (bounded) perturbations can be determined by plugging the decomposition,

$$(U(x,t), V(x,t)) = (\bar{U}, \bar{V}) + (\alpha, \beta)e^{ikx+\lambda t} \text{ with } k \in \mathbb{R}, \lambda \in \mathbb{C}, (\alpha, \beta) \in \mathbb{C}^2, \tag{2.1}$$

into (1.2), followed by linearization. (To have real solutions $(U(x,t), V(x,t))$ of (1.2), one also needs to take complex conjugates into account in (2.1) – see section 2.2.) Of course, the concept of bounded solutions refers to appropriately chosen norms and function spaces; here, we focus on the 'calculus' associated to the Turing destabilization and refer to [41, 45, 70] for a proper functional analytic embedding. The spectral stability of $(\bar{U}, \bar{V})$ is thus determined by the 2×2 linear eigenvalue problem,

$$\mathcal{A}(k;\mu) \begin{pmatrix} \alpha \\ \beta \end{pmatrix} = \begin{pmatrix} g_u - k^2 & g_v \\ h_u & h_v - dk^2 \end{pmatrix} \begin{pmatrix} \alpha \\ \beta \end{pmatrix} = \lambda \begin{pmatrix} \alpha \\ \beta \end{pmatrix} \tag{2.2}$$

with

$$g_u(\mu) = \frac{\partial G}{\partial U}(\bar{U}(\mu), \bar{V}(\mu); \mu), \; g_v(\mu) = \frac{\partial G}{\partial V}(\bar{U}(\mu), \bar{V}(\mu); \mu), \text{ etc.} \tag{2.3}$$

Since $k \in \mathbb{R}$, the associated characteristic polynomial,

$$\lambda^2 - \left[(g_u + h_v) - (1+d)k^2\right]\lambda + \left[(g_u - k^2)(h_v - dk^2) - g_v h_u\right] = 0, \tag{2.4}$$

defines 2 functions $\lambda_{1,2} : \mathbb{R} \to \mathbb{C}$ that are symmetric in k and which we assume to be ordered: $\mathrm{Re}(\lambda_2(k)) \leq \mathrm{Re}(\lambda_1(k))$ – see Fig. 2. The trivial state $(\bar{U}, \bar{V})$ of (1.2) is spectrally stable for those values of the parameter μ for which $\mathrm{Re}(\lambda_{1,2}(k;\mu)) < 0$ for all $k \in \mathbb{R}$. Note that clearly $\lambda_1(k) \sim -dk^2$ and $\lambda_2(k) \sim -k^2$ – or vice versa – as $k \to \infty$, which implies that $(\bar{U}, \bar{V})$ is stable against perturbations (2.1) with sufficiently high wavenumbers k – which of course is a manifestation of the smoothing effect of diffusion. Pattern formation sets in (from $(\bar{U}, \bar{V})$) as μ crosses through a critical value μ_c beyond which there are values of k for which $\mathrm{Re}(\lambda_1(k;\mu)) > 0$. At $\mu = \mu_c$, $(\bar{U}, \bar{V})$ is marginally stable: there is a k_c such that $\mathrm{Re}(\lambda_1(\pm k_c; \mu_c)) = 0$ while $\mathrm{Re}(\lambda_2(k;\mu_c)) \leq 0$ for all $k \in \mathbb{R}$. It follows from the smoothness of $\lambda_{1,2}(k;\mu)$, that $k = k_c$ must be a local maximum of $\mathrm{Re}(\lambda_1(k;\mu_c))$: $\mathrm{Re}(\frac{d\lambda_1}{dk}(\pm k_c;\mu_c)) = 0$ and $\mathrm{Re}(\lambda_1(k;\mu_c)) < 0$ for all k in neighborhoods of $\pm k_c$ – Fig. 2.

If λ is real-valued in a neighborhood of k_c, i.e. if $\lambda_{1,2}(k;\mu) \in \mathbb{R}$ for k near k_c, it follows by taking the derivative with respect to k in (2.4) that $\left[(dg_u + h_v) - 2dk_c^2\right] k_c = 0$ at marginal stability (since $\frac{d\lambda}{dk} = \lambda = 0$ at $(\pm k_c; \mu_c)$). Hence it follows that either $k_c = 0$, or,

$$k_c = k_c(\mu) = \pm\sqrt{\frac{dg_u + h_v}{2d}} \text{ with } dg_u + h_v > 0 \tag{2.5}$$

(Fig. 2(a,b)). If $\lambda_{1,2}(k;\mu) \notin \mathbb{R}$, it follows directly from (2.4) that k_c must be 0 (see Fig. 2(c)) since,

$$\mathrm{Re}(\lambda) = \frac{1}{2}\left[(g_u + h_v) - (1+d)k^2\right]. \tag{2.6}$$

A destabilization that sets in at $k_c = 0$ corresponds directly to a 'homogeneous' bifurcation in the planar *reaction ODE* for (spatially) homogeneous solutions associated to (1.2),

$$\left\{ \begin{array}{rcl} \dot{u} & = & G(u,v;\mu), \\ \dot{v} & = & H(u,v;\mu), \end{array} \right. \tag{2.7}$$

(i.e. with $(U(x,t), V(x,t)) = (u(t), v(t))$), since trivial patterns $(\bar{U}, \bar{V})$ reappear as critical points of (2.7), while their linear stability is – by construction – determined by $\lambda_{1,2}(0;\mu)$ (2.2). In the PDE (1.2), these destabilizations certainly do not necessarily generate 'trivial' homogeneous patterns – see section 2.5 – however, $k_c \neq 0$ – as in Fig. 2(a,b) – is the most natural case to consider if one is interested in the onset of pattern formation. This is the Turing destabilization mechanism that was first proposed by Alan Turing in [83]. Following [83], it is assumed that $\mathrm{Re}(\lambda_{1,2}(0;\mu)) < 0$ so that $(\bar{U}, \bar{V})$ is stable as fixed point of (2.7) – see Fig. 2 (a),(b). This is guaranteed by assuming that

$$g_u + h_v < 0 \ \text{ and } \ g_u h_v - h_u g_v > 0. \tag{2.8}$$

Since $dg_u + h_v > 0$ by (2.5), it follows that destabilization by the Turing mechanism only is possible if,

$$g_u < 0, h_v > 0, g_v h_u < 0, 0 < d < 1 \text{ or } g_u > 0, h_v < 0, g_v h_u < 0, d > 1. \tag{2.9}$$

Note that it thus is necessary for a Turing destabilization that $U(x,t)$ and $V(x,t)$ diffuse with different speeds, i.e. that $d \neq 1$ – see [57] for a further biological interpretation of conditions (2.9) in terms of *activators* and *inhibitors*. Note also that the critical value μ_c of μ is (implicitly) determined by plugging (2.5) back into (2.4), using the fact that $\lambda = 0$ at (k_c, μ_c) (and that $g_u = g_u(\mu)$, etc. (2.3)), which yields,

$$\frac{1}{4d}(dg_u^c - h_v^c)^2 + g_v^c h_u^c = 0, \text{ where } g_u^c = g_u(\mu_c), \text{ etc.}, \tag{2.10}$$

so that, by (2.9),

$$\frac{1}{2}(dg_u^c - h_v^c) = \left\{ \begin{array}{ll} +\sqrt{d|g_v^c h_u^c|} & \text{for} \quad d > 1, \\ -\sqrt{d|g_v^c h_u^c|} & \text{for} \quad 0 < d < 1. \end{array} \right. \tag{2.11}$$

Moreover, it should also be noted that (only) now that the value of μ_c is deduced, the critical wave number k_c of the Turing destabilization can be completely determined (by substituting $\mu = \mu_c$ into (2.5)).

Now let's assume we take μ just beyond μ_c: we set $\mu = \mu_c + \tilde{\mu}\varepsilon^2$ with $0 < \varepsilon^2 \ll 1$ – i.e. $\varepsilon > 0$ is *'sufficiently small'* – and $\tilde{\mu} \in \mathbb{R}$ a scaled bifurcation parameter. For k near k_c, i.e. for $k = k_c + \varepsilon\tilde{k}$, $\lambda_1(k;\mu)$ is expected to be also small and we introduce $\tilde{\lambda}(\tilde{k}, \tilde{\mu})$ by setting $\lambda_1(k;\mu) = \varepsilon^2\tilde{\lambda}(\tilde{k}, \tilde{\mu})$ – note that the assumption that $k - k_c = \varepsilon\tilde{k}$ is based on the anticipated parabolic shape of $\lambda_1(k;\mu)$ near (k_c, μ_c). A straightforward perturbation expansion within (2.4) yields that,

$$\tilde{\lambda}(\tilde{k}, \tilde{\mu}) = \lambda_\mu^c \tilde{\mu} + \frac{1}{2}\lambda_{k^2}^c \tilde{k}^2 + \mathcal{O}(\varepsilon), \tag{2.12}$$

with,

$$\lambda_\mu^c = \frac{\partial \lambda_1}{\partial \mu}(k_c;\mu_c), \ \lambda_{k^2}^c = \frac{\partial^2 \lambda_1}{\partial k^2}(k_c;\mu_c) = \frac{8dk_c^2}{(g_u^c + h_v^c) - (1+d)k_c^2} < 0, \tag{2.13}$$

and a similar (explicit) expression for λ_μ^c which we assume to be $\neq 0$ – as non-degeneracy condition. Thus, $\tilde{\lambda}(\tilde{k}, \tilde{\mu})$ indeed has a parabolic shape, and for $\tilde{\mu}$ such that $\lambda_\mu^c \tilde{\mu} > 0$ there are (spatially periodic) perturbations that grow exponentially. We summarize our (spectral) analysis in the following Lemma.

Lemma 2.1 (Turing destabilization) *Assume that conditions (2.9) hold, let $\mu_c, k_c, \lambda_\mu^c, \lambda_{k^2}^c$ be determined by (2.10), (2.5), (2.13) with $\lambda_\mu^c \neq 0$ (by assumption), and set $\mu = \mu_c + \tilde{\mu}\varepsilon^2$ with $\varepsilon > 0$ sufficiently*

small. Then, the background state $(\bar{U},\bar{V})$ of (1.2) loses stability as $\tilde{\mu}$ crosses through 0: for $\tilde{\mu}\lambda^c_\mu > 0$ there there are two symmetric intervals of unstable wave numbers $k = \pm k_c + \varepsilon\tilde{k}$ with,

$$\tilde{k} \in \left(-\sqrt{\frac{2\lambda^c_\mu \tilde{\mu}}{|\lambda^c_{k^2}|}} + \mathcal{O}(\varepsilon), \sqrt{\frac{2\lambda^c_\mu \tilde{\mu}}{|\lambda^c_{k^2}|}} + \mathcal{O}(\varepsilon) \right), \tag{2.14}$$

such that there exist (real) perturbations of $(\bar{U},\bar{V})$ of the form,

$$e^{i\left(k_c+\varepsilon\tilde{k}\right)x+\varepsilon^2\tilde{\lambda}(\tilde{k},\tilde{\mu})t} \begin{pmatrix} \alpha^c_1 + \mathcal{O}(\varepsilon) \\ \beta^c_1 + \mathcal{O}(\varepsilon) \end{pmatrix} + \text{ c.c.} \tag{2.15}$$

(cf. (2.1)) that grow exponentially, but $\mathcal{O}(\varepsilon^2)$ slow, in time – where (α^c_1, β^c_1) is given in (2.17).

This Lemma describes the Turing <u>destabilization</u> mechanism. At this point it is not clear whether the unstable perturbations (2.15) also evolve into stable (spatially periodic) Turing patterns. We shall show in the upcoming sections that this only is the case if the associated Turing <u>bifurcation</u> is *supercritical*.

Proof. The Lemma follows by a further linear analysis. At (k_c, μ_c), $\mathcal{A}(k;\mu)$ (2.2) is given by,

$$\mathcal{A}(k_c;\mu_c) = \begin{pmatrix} \frac{1}{2d}(dg^c_u - h^c_v) & g_v \\ h_u & -\frac{1}{2}(dg^c_u - h^c_v) \end{pmatrix} = \begin{pmatrix} \pm\sqrt{\frac{|g^c_v h^c_u|}{d}} & g_v \\ h_u & \mp\sqrt{d|g^c_v h^c_u|} \end{pmatrix} \tag{2.16}$$

((2.5),(2.11) and $\pm$ as in (2.11)). This matrix has eigenvalues/eigenvectors,

$$\lambda_1(k_c;\mu_c) = 0, \begin{pmatrix} \alpha^c_1 \\ \beta^c_1 \end{pmatrix} = \begin{pmatrix} \pm\sqrt{|\frac{dg^c_v}{h^c_u}|} \\ 1 \end{pmatrix}, \quad \lambda_2(k_c;\mu_c) = -|d-1|\sqrt{\frac{|g^c_v h^c_u|}{d}}, \begin{pmatrix} \alpha^c_2 \\ \beta^c_2 \end{pmatrix} = \begin{pmatrix} \pm\sqrt{|\frac{g^c_v}{dh^c_u}|} \\ 1 \end{pmatrix} \tag{2.17}$$

– now with $\pm$ according to the sign of $(d-1)h_u$ – which implies (2.15). □

Note that range of the matrix $\mathcal{A}(k_c;\mu_c)$ is (by definition) 1-dimensional and spanned by the vector (α^c_2, β^c_2) – a crucial ingredient in the upcoming derivation of the Ginzburg-Landau equation.

2.2 Nonlinear effects: the derivation of the Ginzburg-Landau equation

'Near onset' – i.e. for $\mu = \mu_c + \varepsilon^2\tilde{\mu}$ and $0 < \varepsilon \ll 1$ sufficiently small – the unstable perturbations associated to Lemma 2.1 can by (2.15) be written as slow (complex) *modulations* of a linearly 'most unstable wave',

$$\left(A_{\text{lin}}(\xi,\tau) \begin{pmatrix} \alpha^c_1 \\ \beta^c_1 \end{pmatrix} E_c(x) + \text{ c.c.} \right) + \text{ h.o.t.}$$

with,

$$\xi = \varepsilon x, \ \tau = \varepsilon^2 t, \ E_c(x) = e^{ik_c x}. \tag{2.18}$$

The basic idea underlying *weakly nonlinear stability theory* is that near onset the nonlinear dynamics of the full PDE (1.2) are also governed by slow modulations of $E_c(x)(\alpha^c_1, \beta^c_1)$, i.e. that there is a complex amplitude $A(\xi,\tau) : \mathbb{R}\times\mathbb{R}^+ \to \mathbb{C}$ such that,

$$\begin{pmatrix} U(x,t) \\ V(x,t) \end{pmatrix} = \begin{pmatrix} \bar{U} \\ \bar{V} \end{pmatrix} + \varepsilon A(\xi,\tau) \begin{pmatrix} \alpha^c_1 \\ \beta^c_1 \end{pmatrix} E_c(x) + \text{ c.c. } + \mathcal{O}(\varepsilon^2), \tag{2.19}$$

where we thus made an explicit choice for the amplitude of these perturbations: we have assumed them to be of order $\varepsilon \sim \sqrt{|\mu - \mu_c|}$. The intuitive motivation for this choice lies in the observation that the Fourier-nature of (2.19) implies that quadratic 'interactions' will generate the 'higher harmonics' $\varepsilon^2 E_c^2$, $\varepsilon^2 E_c^0$, and $\varepsilon^2 E_c^{-2}$ and thus will not directly couple back to the original E_c-mode. This can only happen at the next – cubic – level. Choosing an $\mathcal{O}(\varepsilon)$ amplitude implies that the nonlinear interactions indeed may 'balance' the temporal evolution – that also acts on the $\varepsilon^3 E_c$ level (since $\frac{\partial}{\partial t}(U,V) \sim \varepsilon^3 A_\tau E_c(\alpha^c_1, \beta^c_1) +$

c.c.). Thus, it is natural to expect that nonlinear effects indeed may counteract the destabilization if the perturbations have grown to an $\mathcal{O}(\varepsilon)$ amplitude.

The evolution of $A(\xi,\tau)$ can now be determined explicitly by refining (2.19) into the 'Ansatz',

$$\begin{aligned}\begin{pmatrix} U-\bar{U} \\ V-\bar{V} \end{pmatrix} = E_c[\varepsilon A \begin{pmatrix} \alpha_1^c \\ \beta_1^c \end{pmatrix} &+ E_c^0[\varepsilon^2 \begin{pmatrix} X_{02} \\ Y_{02} \end{pmatrix} + \varepsilon^3 \begin{pmatrix} X_{03} \\ Y_{03} \end{pmatrix} + \mathcal{O}(\varepsilon^4)] \\ &+ \varepsilon^2 \begin{pmatrix} X_{12} \\ Y_{12} \end{pmatrix} + \varepsilon^3 \begin{pmatrix} X_{13} \\ Y_{13} \end{pmatrix} + \mathcal{O}(\varepsilon^4)] \\ &+ E_c^2[\varepsilon^2 \begin{pmatrix} X_{22} \\ Y_{22} \end{pmatrix} + \varepsilon^3 \begin{pmatrix} X_{23} \\ Y_{23} \end{pmatrix} + \mathcal{O}(\varepsilon^4)] \\ &+ E_c^3[\varepsilon^3 \begin{pmatrix} X_{33} \\ Y_{33} \end{pmatrix} + \mathcal{O}(\varepsilon^4)] \\ &+ \text{h.o.t.} + \text{c.c.}\end{aligned} \tag{2.20}$$

in which the vector fields $(X_{ij}(\xi,\tau), Y_{ij}(\xi,\tau))$ can be determined by substitution of (2.20) into (1.2) and gathering together all terms at the $\varepsilon^j E_c^i$ levels. Since,

$$\frac{\partial}{\partial t}(\varepsilon[AE_c]) = \varepsilon^3 A_\tau E_c, \quad \frac{\partial^2}{\partial x^2}(\varepsilon[AE_c]) = \varepsilon[-k_c^2 A + 2i\varepsilon k_c A_\xi + \varepsilon^2 A_{\xi\xi}]E_c, \tag{2.21}$$

it follows that the $\varepsilon^2 E_c^0$ and $\varepsilon^2 E_c^2$ levels can only be reached through quadratic nonlinearities originating from the Taylor expansions of $G(U,V)$ and $H(U,V)$ around $(\bar{U},\bar{V})$,

$$G = (g_u^c U + g_v^c V) + (\frac{1}{2}g_{u^2}^c U^2 + g_{uv}^c UV + \frac{1}{2}g_{v^2}^c V^2) + (\frac{1}{6}g_{u^3}^c U^3 + \frac{1}{2}g_{u^2v}^c U^2 V + \frac{1}{2}g_{uv^2}^c UV^2 + \frac{1}{6}g_{v^3}^c V^3) + \mathcal{O}(4) \tag{2.22}$$

– with $g_{u^2}^c$ etc. as in (2.3), (2.10). This yields the following equations for (X_{02}, Y_{02}) and (X_{22}, Y_{22}),

$$\mathcal{A}(0;\mu_c)\begin{pmatrix} X_{02} \\ Y_{02} \end{pmatrix} = |A|^2 \begin{pmatrix} \bar{X}_{02} \\ \bar{Y}_{02} \end{pmatrix}, \quad \mathcal{A}(2k_c;\mu_c)\begin{pmatrix} X_{02} \\ Y_{02} \end{pmatrix} = A^2 \begin{pmatrix} \bar{X}_{22} \\ \bar{Y}_{22} \end{pmatrix}, \tag{2.23}$$

– with $\mathcal{A}(k;\mu)$ from (2.2) – where the constants $\bar{X}_{02}, \bar{X}_{22}, \bar{Y}_{02}, \bar{Y}_{22} \in \mathbb{R}$ are explicitly known as (usually quite involved) expressions in g_u^c, g_v^c, h_u^c, h_v^c, $g_{u^2}^c$, g_{uv}^c, $g_{v^2}^c$, $h_{u^2}^c$, h_{uv}^c, $h_{v^2}^c$ and μ_c. By construction – or: since we consider the Turing bifurcation – neither $\mathcal{A}(0;\mu_c)$ nor $\mathcal{A}(2;\mu_c)$ can have an eigenvalue $\lambda(\mu_c) = 0$ (Fig. 2) which implies that (X_{02}, Y_{02}) and (X_{22}, Y_{22}) are determined uniquely,

$$\begin{pmatrix} X_{02}(\xi,\tau) \\ Y_{02}(\xi,\tau) \end{pmatrix} = |A|^2(\xi,\tau)\begin{pmatrix} \alpha_{02} \\ \beta_{02} \end{pmatrix}, \quad \begin{pmatrix} X_{22}(\xi,\tau) \\ Y_{22}(\xi,\tau) \end{pmatrix} = A^2(\xi,\tau)\begin{pmatrix} \alpha_{22} \\ \beta_{22} \end{pmatrix} \tag{2.24}$$

for certain $\alpha_{02}, \alpha_{22}, \beta_{02}, \beta_{22} \in \mathbb{R}$. Thus, as functions of ξ and τ, $(X_{02,22}, Y_{02,22})$ are 'slaved' to amplitude $A(\xi,\tau)$. This is very different at the E_c^1 levels. First, we note that the equation appearing at the leading εE_c level is satisfied *by construction*: it 'confirms' the linear stability analysis of section 2.1. At $\varepsilon^2 E_c$ we find by (2.17), (2.21) that,

$$\mathcal{A}(k_c;\mu_c)\begin{pmatrix} X_{12} \\ Y_{12} \end{pmatrix} = 2ik_c A_\xi \begin{pmatrix} \alpha_1^c \\ d\beta_1^c \end{pmatrix} = 2idk_c A_\xi \begin{pmatrix} \alpha_2^c \\ \beta_2^c \end{pmatrix}. \tag{2.25}$$

Thus, although $\mathcal{A}(k_c;\mu_c)$ is not invertible (since $\lambda_1(k_c,\mu_c) = 0$ by (2.17)), (2.25) can be solved,

$$\begin{pmatrix} X_{12}(\xi,\tau) \\ Y_{12}(\xi,\tau) \end{pmatrix} = -2i\frac{d^2 k_c}{|d-1|\sqrt{d|g_v^c h_u^c|}} A_\xi(\xi,\tau)\begin{pmatrix} \alpha_2^c \\ \beta_2^c \end{pmatrix} + A_1(\xi,\tau)\begin{pmatrix} \alpha_1^c \\ \beta_1^c \end{pmatrix}. \tag{2.26}$$

Naturally, the solution is not uniquely determined, with the 'higher order amplitude' $A_1(\xi,\tau)$ we have introduced another unknown function. By construction, everything comes together at the next level,

$$\mathcal{A}(k_c;\mu_c)\begin{pmatrix} X_{13} \\ Y_{13} \end{pmatrix} = \begin{pmatrix} \alpha_1^c A_\tau + \bar{X}_{13}^{\text{inst}}\tilde{\mu}A + \bar{X}_{13}^{\text{diff}} A_{\xi\xi} + \bar{X}_{13}^{\text{nl}} A|A|^2 \\ \beta_1^c A_\tau + \bar{Y}_{13}^{\text{inst}}\tilde{\mu}A + \bar{Y}_{13}^{\text{diff}} A_{\xi\xi} + \bar{Y}_{13}^{\text{nl}} A|A|^2 \end{pmatrix} + 2idk_c A_{1,\xi}\begin{pmatrix} \alpha_2^c \\ \beta_2^c \end{pmatrix}, \tag{2.27}$$

where all $\bar{X}_{13}^{\text{inst}}, \bar{X}_{13}^{\text{diff}}, \bar{X}_{13}^{\text{nl}}, \bar{Y}_{13}^{\text{inst}}, \bar{Y}_{13}^{\text{diff}}, \bar{Y}_{13}^{\text{nl}} \in \mathbb{R}$ can be determined explicitly – although it should be remarked that especially $\bar{X}_{13}^{\text{nl}}, \bar{Y}_{13}^{\text{nl}}$ are highly involved expressions in terms of the quadratic and cubic Taylor coefficients of $G(U,V;\mu)$ and $H(U,V;\mu)$ (2.22). Once again, $\mathcal{A}(k_c;\mu_c)$ is not invertible, there can only be a solution (X_{13}, Y_{13}) if the right-hand side of (2.27) satisfies a solvability/Fredholm condition, i.e. if,

$$\pm\left(\alpha_1^c A_\tau + \bar{X}_{13}^{\text{inst}}\tilde{\mu}A + \bar{X}_{13}^{\text{diff}}A_{\xi\xi} + \bar{X}_{13}^{\text{nl}}A|A|^2\right) = \sqrt{|\frac{g_v^c}{dh_u^c}|}\left(\beta_1^c A_\tau + \bar{Y}_{13}^{\text{inst}}\tilde{\mu}A + \bar{Y}_{13}^{\text{diff}}A_{\xi\xi} + \bar{Y}_{13}^{\text{nl}}A|A|^2\right), \tag{2.28}$$

(by (2.17)) – with $\pm$ according to the sign of $(d-1)h_u$. This relation between A_τ, $\tilde{\mu}A$, $A_{\xi\xi}$ and $A|A|^2$ can be written as the *Ginzburg-Landau equation*,

$$A_\tau = -\frac{1}{2}\lambda_{k^2}^c A_{\xi\xi} + \tilde{\mu}\lambda_\mu^c A + LA|A|^2 \tag{2.29}$$

with λ_μ^c and $\lambda_{k^2}^c$ as defined in (2.13) – recall $\lambda_{k^2}^c < 0$ – and $L \in \mathbb{R}$ the *Landau coefficient*. (We refer to Remark 2.6 for more background on the Ginzburg-Landau equation.) Note that it is not obvious from (2.28) that the terms λ_μ^c and $\lambda_{k^2}^c$ – see Lemma 2.1 – must (re-)appear, but carefully tracing the components leading to the linear terms in (2.29) confirms that this necessarily is the case. In practice, it is a good check against computational errors and thus a valuable 'anchor' in the derivation of the correct expression for L (which is in general quite a task). The value of L and especially its sign is crucial: *the Turing bifurcation that yields Turing patterns only takes place if* $L < 0$, as we show in section 2.4. In fact, there we show that no (small amplitude) Turing patterns can exist beyond the Turing destabilization if $L > 0$.

Nevertheless, we refrain from giving an explicit expression for L – we are not aware of such an expression in the literature. In [69], a version of (1.2) is considered with $0 < d < 1$ and,

$$G(U,V) = \mu U + V + a_1U^2 + a_2UV + a_3V^2 + a_4U^3,\ H(U,V) = -U + \nu V + b_1U^2 + b_2UV + b_3V^2 + b_4V^3, \tag{2.30}$$

so that $(\bar{U},\bar{V}) = (0,0)$. Thus, in the setting of the present weakly nonlinear stability analysis, the system considered in [69] corresponds to (1.2) with parameter μ only appearing in g_u^c, and with $g_v^c = 1$, $h_u^c = -1$ and $g_{u^2v}^c = g_{uv^2}^c = g_{v^3}^c = h_{u^3}^c = h_{u^2v}^c = h_{uv^2}^c = 0$. It follows – either from section 2.1 or from [69] – that,

$$k_c = \sqrt{\frac{\nu - \sqrt{d}}{d}},\ \mu_c = \frac{\nu - 2\sqrt{d}}{d},\ \mathcal{A}(k_c;\mu_c) = \begin{pmatrix} -\frac{1}{\sqrt{d}} & 1 \\ -1 & \sqrt{d} \end{pmatrix},\ \begin{pmatrix} \alpha_1^c \\ \beta_1^c \end{pmatrix} = \begin{pmatrix} \sqrt{d} \\ 1 \end{pmatrix} \tag{2.31}$$

for second parameter $\nu = h_v^c \in (\sqrt{d}, 2\sqrt{d}/(1+d))$. (Note that $k_c \downarrow 0$ as $\nu \to \sqrt{d}$, that the transition from the 'fully real' case of Fig. 2 (a) to the partly complex case in (b) occurs at $\nu = 2\sqrt{d}/(1+\sqrt{d}) \in (\sqrt{d}, 2\sqrt{d}/(1+d))$, and that a Hopf bifurcation takes place in the reaction ODE as $\nu \uparrow 2\sqrt{d}/(1+d)$) – i.e. it marks the transition from Fig. 2 (b) to (c).) In [69], the Ginzburg-Landau equation that describes the evolution of small $\mathcal{O}(\varepsilon)$ patterns for $\mu = \mu_c + \tilde{\mu}\varepsilon^2$ is given by,

$$A_\tau = \frac{4d(\nu - \sqrt{d})}{1-d}A_{\xi\xi} - \frac{d}{1-d}\tilde{\mu}A + LA|A|^2, \tag{2.32}$$

which indeed agrees with the general form (2.29); the expression for L is given by (3.6)-(3.11) in [69]. If one assumes that $a_2 = a_3 = b_2 = b_3 = 0$ – i.e. if the nonlinear parts of $G(U,V)$, respectively $H(U,V)$, only consist of $a_1U^2 + a_4U^3$, resp. $b_1V^2 + b_4V^3$ – the expression for L reduces to,

$$L = L(\nu, a_1, a_4, b_1, b_4) = \frac{2d^2\sqrt{d}(\sqrt{d}a_1 - b_1)\left((15\nu + 4\sqrt{d})a_1 - 19b_1\right)}{9(1-d)(\nu - \sqrt{d})^2} - \frac{3d^2a_4 - b_4}{(1-d)}. \tag{2.33}$$

Thus, we conclude that L is explicitly determined by quadratic coefficients a_1, b_1 and cubic coefficients a_4, b_4 of Taylor expansions (2.22). Specifically, the sign of L may change by varying either one of these.

Remark 2.2 The number of reaction-diffusion models for which the Ginzburg-Landau equation that governs the bifurcation of Turing patterns has been explicitly determined is relatively limited, see for instance [49], [55] and [85] for the Brusselator, Gray-Scott, and extended Klausmeier models. More typically, the nature of the Turing bifurcation – and thus implicitly the sign of L (section 2.4) is determined by numerical path following methods for specific choices of the parameters – see for instance [97].

2.3 The validity of the Ginzburg-Landau approximation

Although the validity of the Ginzburg-Landau approximation is essential for the relevance of its derivation and more importantly for the dynamics of the full, underlying equation (1.2) – or more generally (1.1) – we do not go into the details of this issue. We only sketch the main ideas – without going into the functional analytic aspects of the theory. First, we note that there are two aspects to the validity of the Ginzburg-Landau approximation.

• **The validity of the Ginzburg-Landau dynamics on finite time-scales.** Let $A(\xi,\tau)$ be a solution of Ginzburg-Landau equation (2.29) with initial condition $A(\xi,0)=A_0(\xi)$. Note that we a priori cannot expect this solution to exist for all time – in fact, the Ginzburg-Landau equation is known to have solutions that blow up in finite time if $L>0$ [2, 54]. Nevertheless, we may assume that there is a $T>0$ such that $A(\xi,\tau)$ exists as solution of (2.29) for $\tau\in(0,T)$ (in some Banach space X). Through Ansatz (2.20) and the 'slaving relations' (2.24) and (2.26), we thus have a potential approximation $(U_{\rm GL}(x,t),V_{\rm GL}(x,t))$ of a solution $(U(x,t),V(x,t))$ of the original underlying system (1.2). More specifically, we may define $(U_{\rm GL}(x,t),V_{\rm GL}(x,t))$ through the $\mathcal{O}(1)$, $\mathcal{O}(\varepsilon)$ and $\mathcal{O}(\varepsilon^2)$ terms in (2.20) that are all explicitly given in terms of $A(\xi,\tau)$ by (2.24) and (2.26) (setting $A_1(\xi,\tau)\equiv 0$; note that one may in principle obtain an approximation $(U_{\rm GL}(x,t),V_{\rm GL}(x,t))$ that is accurate up to $\mathcal{O}(\varepsilon^j)$ for any (finite) $j>0$ by further elaborating the approximation set up by (2.20)). It is natural to expect that $(U_{\rm GL}(x,t),V_{\rm GL}(x,t))$ 'encodes precise information' about solutions $(U(x,t),V(x,t))$ of (1.2). The finite-time validity question now is: *If we consider a solution $(U(x,t),V(x,t))$ of (1.2) that has initial conditions $\mathcal{O}(\varepsilon^2)$ close to those of $(U_{\rm GL}(x,t),V_{\rm GL}(x,t))$ (that are determined by $A_0(\xi)$) – i.e. if $\|(U(x,0)-U_{\rm GL}(x,0),V(x,0)-V_{\rm GL}(x,0))\|=\mathcal{O}(\varepsilon^2)$ (in some appropriate norm $\|.\|_X$) – does $(U(x,t),V(x,t))$ remain $\mathcal{O}(\varepsilon^2)$ close to $(U_{\rm GL}(x,t),V_{\rm GL}(x,t))$ for all $t\in(0,T/\varepsilon^2)$, i.e. is the approximation valid/asymptotically accurate on the long $\mathcal{O}(1/\varepsilon^2)$ ($\tau-$) time scale associated to the Ginzburg-Landau equation?* Roughly speaking, the answer to this question is yes, although it should be noted that establishing this issue has been an open problem for about 20 years – see Remark 2.6. The above formulation of the validity issue is insufficiently precise, it's exactly the choice(s) of suitable Banach space(s) X, etc. – the aspect we completely evade here – that is crucial for 'controlling' the validity/asymptotic accuracy of the Ginzburg-Landau approximation scheme. We refer to [54] for an extended treatment, including all relevant details.

• **Persistence of asymptotically stable solutions for all t.** Consider a specific – *special* – solution $A^*(\xi,\tau)$ of (2.29) for which we – by assumption – have been able to show that it is asymptotically stable (these are typically the spatially periodic solutions of (2.29) – see section 2.4 and Remark 2.6). By the above described procedure, we can associate an approximate solution $(U^*_{\rm GL}(x,t),V^*_{\rm GL}(x,t))$ of (1.2) to $A^*(\xi,\tau)$. Now the question is: *Is there an – again special – solution $(U^*(x,t),V^*(x,t))$ of (1.2) that is $\mathcal{O}(\varepsilon^2)$ close to $(U^*_{\rm GL}(x,t),V^*_{\rm GL}(x,t))$ that exists for all t and that is asymptotically stable as solution of (1.2)?* Given the finite-time validity result and the structure of the Ginzburg-Landau approximation procedure, one would intuitively expect this to be the case. Again, this is correct – roughly speaking. Once more, it is crucial to precisely formulate the setting and to carefully choose spaces and norms, and once more we do not go into details here. Nevertheless, in practice one may work with the rule of thumb that any asymptotically stable solution $A^*(\xi,\tau)$ of Ginzburg-Landau equation (2.29) indeed corresponds to an asymptotically stable small amplitude solution $(U^*(x,t),V^*(x,t))$ of (1.2). See also the upcoming Theorem 2.4.

We also note that it is a priori not clear that all small amplitude patterns near a trivial state 'at onset' will be governed by solutions of the type $(U_{\rm GL}(x,t),V_{\rm GL}(x,t))$, i.e. solutions that are driven by the Ginzburg-Landau equation: a general perturbation of the trivial pattern $(\bar U,\bar V)$ of (1.2) does not necessarily have the structure of (2.19) or of Ansatz (2.20). However, it can be shown that near a Turing destabilization general perturbations will evolve towards the mixed asymptotic/Fourier expansion described by (2.20) on a time scale that is faster than the $\mathcal{O}(1/\varepsilon^2)$ time scale of the Ginzburg-Landau dynamics – see [5, 30].

Thus, in situations where the trivial pattern $(\bar U,\bar V)$ of (1.2) undergoes a Turing destabilization at $\mu=\mu_c$, one may conclude that for $|\mu-\mu_c|=\mathcal{O}(\varepsilon^2)$ – and $0<\varepsilon\ll 1$ 'sufficiently small' – the full dynamics of the flow generated by (1.2) in an $\mathcal{O}(\varepsilon)$ neighborhood of $(\bar U,\bar V)$ – in a certain norm – is driven by the Ginzburg-Landau approximation (2.29) on a time scale of $\mathcal{O}(1/\varepsilon^2)$. Beyond this time scale, no such general validity result 'for all solutions' exists (and can in fact in general also not be correct). However, any 'special' asymptotically stable solution of (2.29) persists as an asymptotically stable solution of the full system (1.2), it thus must also exist for all $t>0$.

2.4 Ginzburg-Landau dynamics and the Turing bifurcation

To study the dynamics generated by Ginzburg-Landau equation (2.29), we simplify it by rescaling, of course first (and most importantly) under the assumption that that Lemma 2.1 holds, i.e. that the trivial pattern $(\bar{U}, \bar{V})$ of (1.2) – that corresponds to $A(\xi, \tau) \equiv 0$ in (2.29) – has been destabilized by the Turing mechanism. By introducing,

$$\hat{\tau} = \tilde{\mu}\lambda_{\mu}^{c}\tau, \quad \hat{\xi} = \sqrt{\frac{2\tilde{\mu}\lambda_{\mu}^{c}}{|\lambda_{k^2}^{c}|}}\xi, \quad \hat{A} = \sqrt{\frac{|L|}{\tilde{\mu}\lambda_{\mu}^{c}}}A, \tag{2.34}$$

and immediately dropping the 'hats' again, (2.29) becomes,

$$A_{\tau} = A_{\xi\xi} + A \pm A|A|^2, \tag{2.35}$$

with $\pm$ according to the sign of the Landau coefficient L. The case $L < 0$ – i.e. $-A|A|^2$ in (2.35) – corresponds to the *supercritical Turing bifurcation*; $L > 0$ is the subcritical case (see Remark 2.5). In the supercritical case there is a one-parameter family – a 'band' – of (stationary) spatially periodic solutions $A(\xi, \tau) = Re^{iK\xi}$ (and $R \geq 0$) with,

$$K^2 + R^2 = 1 \text{ and } -1 < K < 1. \tag{2.36}$$

By rescaling (2.34), this interval corresponds directly to the band of spectrally unstable waves of Lemma 2.1 (2.14): in the supercritical case, the Ginzburg-Landau formalism indeed couples a finite-amplitude spatially periodic pattern to each of the spectrally unstable waves generated by the Turing destabilization. However, not all of these patterns are stable, as is the statement of the celebrated Eckhaus/Benjamin-Feir-Newell criterion.

Lemma 2.3 (Eckhaus/Benjamin-Feir-Newell) *The periodic solution $A(\xi, \tau) = Re^{iK\xi}$ of (2.35), with (R, K) as in (2.36), is spectrally stable for $-1/\sqrt{3} < K < 1/\sqrt{3}$ and unstable for $|K| \in (1/\sqrt{3}, 1)$.*

In fact, this is a special version of the criterion for the case that the coefficients of the Ginzburg-Landau equation (2.29)/(2.35) are all real valued – as is necessary the case for a Turing bifurcation in a 2-component reaction-diffusion equation, see Lemma 2.7 and Remarks 2.6, 3.2.

Proof of Lemma 2.3. This result is obtained by a straightforward spectral stability analysis in the spirit of section 2.1. However, since the solution we're linearizing about is not a trivial state, we add an additional ingredient: we 'decouple' the spatial dynamics of the underlying pattern $Re^{iK\xi}$ by moving along with it, i.e. we set without loss of generality,

$$A(\xi, \tau) = Re^{iK\xi} + B(\xi, \tau)e^{iK\xi} = (R + B(\xi, \tau)))e^{iK\xi}$$

– so that the behavior of $B \in \mathbb{C}$ determines the stability of $Re^{iK\xi}$ – substitute this into (2.35) and linearize,

$$B_{\tau} = B_{\xi\xi} + 2iKB_{\xi} - R^2\left(B + \bar{B}\right) \tag{2.37}$$

(where we have used (2.36)). Decomposing $B(\xi, \tau)$ into real and imaginary parts – i.e. setting $B(\xi, \tau) = U(\xi, \tau) + iV(\xi, \tau)$ (thus with $U, V \in \mathbb{R}$) – yields a linear system that looks quite familiar,

$$\left\{ \begin{array}{rcrcrcr} U_{\tau} & = & U_{\xi\xi} & - & 2KV_{\xi} & - & 2R^2U, \\ V_{\tau} & = & V_{\xi\xi} & + & 2KU_{\xi} & & \end{array} \right. \tag{2.38}$$

(although we didn't have the 'advection terms' U_{ξ} and V_{ξ} in section 2.1). Thus, we set $(U(\xi, \tau), V(\xi, \tau)) = (\alpha, \beta)e^{ik\xi + \lambda\tau}$ with $k \in \mathbb{R}$ and $\lambda = \lambda(k) \in \mathbb{C}$ (cf. (2.1)) and obtain,

$$\begin{pmatrix} -2R^2 - k^2 & -2ikK \\ 2ikK & -k^2 \end{pmatrix} \begin{pmatrix} \alpha \\ \beta \end{pmatrix} = \lambda \begin{pmatrix} \alpha \\ \beta \end{pmatrix}, \tag{2.39}$$

which yields $\lambda^2 + 2\lambda(k^2 + R^2) + (2R^2 - 4K^2 + k^2)k^2 = 0$. Thus, $A(\xi, \tau)$ is spectrally stable if,

$$\lambda_1 + \lambda_2 = -2(k^2 + R^2) < 0 \text{ and } \lambda_1\lambda_2 = 2(1 - 3K^2 + \frac{1}{2}k^2)k^2 \geq 0 \text{ for all } k \in \mathbb{R} \tag{2.40}$$

(2.36), which indeed is equivalent to the Eckhaus/Benjamin-Feir-Newell stability criterion. □

The mechanism by which the unstable spatially periodic 'wave trains' are destabilized is called *the sideband instability.* This name comes from the observation that the 'most unstable' perturbations are those with wave numbers $k \to 0$ – the 'sidebands' – see (2.40), and consider especially the critical waves with $K = \pm 1/\sqrt{3}$, that must have $\lambda_1(0) = \frac{d\lambda_1}{dk}(0) = \frac{d^2\lambda_1}{dk^2}(0) = \frac{d^3\lambda_1}{dk^3}(0) = 0$ (since clearly $\lambda_2(k) = -2R^2 + \mathcal{O}(k^2)$ for $|k| \ll 1$ – see also (2.45) in the proof of Lemma 2.7 in section 2.5.1).

Thus, we may now conclude – also by the validity results discussed in section 2.3 – that *if the Landau coefficient L in the Ginzburg-Landau approximation (2.29) is negative*, the Turing destabilization of Lemma 2.1 indeed yields the appearance of a band of spatially periodic small amplitude patterns with wave lengths centered around k_c.

Theorem 2.4 (The Turing bifurcation) *Let the conditions and definitions of Lemma 2.1 hold. For Landau coefficient $L < 0$ – with L given in Ginzburg-Landau equation (2.29) and determined in section 2.2 – and $0 < \varepsilon \ll 1$ sufficiently small, a Turing bifurcation takes place as $\tilde{\mu}$ crosses through 0: for $\tilde{\mu}\lambda_\mu^c > 0$ there exists a continuous band – the Eckhaus band – of asymptotically stable stationary spatially periodic patterns $(U_p(x;k), V_p(x;k))$ of (1.2) with wave number k centered around k_c,*

$$k = k(K) = k_c + \varepsilon\sqrt{\frac{2\tilde{\mu}\lambda_\mu^c}{|\lambda_{k^2}^c|}}K, \tag{2.41}$$

and $-1/\sqrt{3} + \mathcal{O}(\varepsilon) < K < 1/\sqrt{3} + \mathcal{O}(\varepsilon)$. The patterns $(U_p(x;k), V_p(x;k))$ are $\mathcal{O}(\varepsilon)$ close to the (destabilized) background state $(\bar{U}, \bar{V})$ and are – for any phase shift $\theta \in \mathbb{R}$ – approximated by,

$$\begin{pmatrix} U_p(x;k,\theta) \\ V_p(x;k,\theta) \end{pmatrix} = \begin{pmatrix} \bar{U} \\ \bar{V} \end{pmatrix} + \varepsilon\left(\sqrt{1-K^2} + \mathcal{O}(\varepsilon)\right)\sqrt{\frac{\tilde{\mu}\lambda_\mu^c}{|L|}}\begin{pmatrix} \alpha_1^c\cos(k(K)x+\theta) + \mathcal{O}(\varepsilon) \\ \beta_1^c\cos(k(K)x+\theta) + \mathcal{O}(\varepsilon) \end{pmatrix}.$$

As was already noted in section 2.3, the $\mathcal{O}(\varepsilon)$ corrections in the statement of the Theorem can in principle be explicitly determined by further elaboration of the approximation scheme set up by (2.20).

The analysis in this and the preceding sections provides the backbone of a proof of this Theorem, however, we refrain from going into the details here – see section 2.3. We – for instance – refer to [55] in which the abstract results of the review [72] on the Ginzburg-Landau procedure have been applied to establish the appearance of spatially periodic small amplitude patterns at the Turing bifurcation in the Gray-Scott model.

Once more, we stress that even in the above case of a supercritical Turing bifurcation, the 'predictions' of the linear analysis of Lemma 2.1 are not completely 'confirmed' by the nonlinear analysis: only the Eckhaus subband of the band of exponentially growing spatially periodic patterns (2.14) – described by the Eckhaus/Benjamin-Feir-Newell stability criterion/Lemma 2.3 – appears as stable – and thus 'observable' – Turing patterns. As expected, in the subcritical case, i.e. if $L > 0$, the exponential growth of the linearly unstable modes is not balanced by nonlinear effects and *the Turing destabilization does not imply the existence of spatially periodic small amplitude Turing patterns.*

In fact, the Ginzburg-Landau formalism does provide a – more precisely: two – unbounded band(s) of spatially periodic patterns in the subcritical case, i.e. in the version of (2.35) with the $+A|A|^2$-term: again setting $A(\xi, \tau) = Re^{iK\xi}$ yields $K^2 - R^2 = 1$ (cf. (2.36)). However, these patterns are all unstable, as can be seen directly by following the spectral analysis in the proof of Lemma 2.3: the equivalent of (2.37) for the subcritical case is, $B_\tau = B_{\xi\xi} + 2iKB_\xi + R^2\left(B + \bar{B}\right)$, which yields that $\lambda_1 + \lambda_2 = -2(k^2 - R^2) = 2(R^2 - k^2)$ in (2.40), which is positive for $|k| < R$.

Finally, we note that (slightly) before the onset of the Turing bifurcation, i.e. if $\tilde{\mu}\lambda_\mu^c < 0$ in (2.29), there exists a spatially periodic pattern of the form $A(\xi, \tau) = Re^{iK\xi}$ for all $K \in \mathbb{R}$ in the subcritical case (as is straightforward to check). However, it can directly be checked that also these patterns are spectrally unstable. As expected, there are no such spatially periodic patterns in the supercritical case.

Remark 2.5 The case $L = 0$ can be studied as co-dimension 2 bifurcation by assuming that there is a second independent parameter $\nu \in \mathbb{R}$ in the underlying problem so that $L = L(\nu)$, with ν_c such that $L(\nu_c) = 0$ – see for instance (2.33). In that case, the dynamics of small-amplitude patterns is governed by the *degenerate Ginzburg-Landau equation* that contains additional terms like $|A|^2 A_\xi$, $A^2 \bar{A}_\xi$, and $A|A|^4$ (compared to (2.35)) – see [16, 75] for the dynamics generated by this equation and its validity.

Remark 2.6 The first explicit derivations of the Ginzburg-Landau equation as modulation equation – in the setting of fluid mechanics – appeared in [14, 59, 79], only about 20 years later followed by the first validity proofs of the Ginzburg-Landau approximation formalism [12, 86] (a first derivation of a Ginzburg-Landau equation in the context of 2-component RDEs appeared in [50]). The Eckhaus/Benjamin-Feir-Newell stability criterion originates from [4, 29, 58, 80], a first nonlinear stability result was established in [44]. See the review papers [2, 54].

2.5 Alternative pattern generating mechanisms near equilibrium

2.5.1 The Hopf bifurcation

A spectral analysis as in section 2.1 indicates that a Hopf bifurcation in the reaction ODE (2.7) also generates patterns: as μ passes through the critical value μ_c, there is again a band of wave numbers (centered around $k_c = 0$) associated to exponentially growing – and thus unstable – perturbations of the form (2.1) – see Fig. 2(c). Even if it is known whether the Hopf bifurcation is super- or subcritical in ODE (2.7), a weakly nonlinear Ginzburg-Landau analysis is necessary to ensure the existence – or not – of stable small amplitude patterns. The formalism is identical to that of the Turing bifurcation in section 2.2, i.e. it follows the Ansatz (2.20), with two differences: the critical wave E_c is a function of time, $E_c = E_c(t) = e^{i\omega_c t}$ with $i\omega_c = \lambda_1(0; \mu_c) \in i\mathbb{R}$ (cf. (2.18)), and $(\alpha_1^c, \beta_1^c), (X_{ij}, Y_{ij}) \in \mathbb{C}^2$ in (2.20). Eventually, the procedure results in the *complex Ginzburg-Landau equation*,

$$A_\tau = -\frac{1}{2}\lambda_{k^2}^c A_{\xi\xi} + \tilde{\mu}\lambda_\mu^c A + LA|A|^2 \ \text{ with } \ \lambda_{k^2}^c, \lambda_\mu^c, L \in \mathbb{C} \tag{2.42}$$

(cf. (2.29)). As in the Turing case, it can be shown that the Ginzburg-Landau approximation scheme is valid for all solutions on a bounded τ-interval, i.e. an $\mathcal{O}(1/\varepsilon^2)$ t-interval in (1.2) [71] and that asymptotically stable solutions of (2.42) correspond to asymptotically stable patterns in (1.2) (that exist for all t) – see section 2.3. By scaling A, ξ and τ as in section 2.4, in combination with an additional transformation $A \to e^{i\hat{\omega}t}\hat{A}$ for a well-chosen $\hat{\omega}$, (2.43) can be brought into the form,

$$A_\tau = (1 + ia)A_{\xi\xi} + A \pm (1 + ib)A|A|^2, \ \text{ with } \ a, b \in \mathbb{R}, \tag{2.43}$$

with $\pm$ determined by the sign of $\mathrm{Re}(L)$. Compared to the (scaled) real Ginzburg-Landau equation (2.35), there are two real parameters, a and b of which b is determined by the imaginary part of the Landau coefficient L. For simplicity, we now only consider the supercritical case $\mathrm{Re}(L) < 0$, i.e. $\pm \to -$ in (2.43), and search for simple 'plane waves': we subsitute $A(\xi, \tau) = Re^{i(K\xi + W\tau)}$ into (2.43) and find a generalization of (2.36),

$$K^2 + R^2 = 1, \ W = -aK^2 - bR^2 \text{ and } -1 < K < 1. \tag{2.44}$$

Thus, any choice of $K \in (-1, 1)$ uniquely determines a $R(K)$ and a $W(K)$ – a situation very similar to the real case. As in the real case – Lemma 2.3 – one expects only a subband to be stable against sideband perturbations, however this subband shrinks to the empty set as $1 + ab$ becomes negative.

Lemma 2.7 (Eckhaus/Benjamin-Feir-Newell for the complex Ginzburg-Landa equation) *The spatially periodic solution $A(\xi, \tau) = Re^{i(K\xi + W\tau)}$ of (2.35) – with (R, K, W) as in (2.44) – is stable against sideband perturbations if $K \in (-1, 1)$ is such that $(1 + ab)(1 - K^2) - 2(1 + b^2)K^2 > 0$, and unstable otherwise. Hence, neither of these plane wave solutions can be stable if $1 + ab < 0$.*

Thus, the width of the Eckhaus-stable subband – that is $2/\sqrt{3}$ in the real case $a = b = 0$ (Lemma 2.3) – shrinks to 0 as $1 + ab \downarrow 0$, so that neither of the exponentially growing periodic perturbations described by the linear analysis – that are directly associated to the planes waves (2.44) (as in the Turing case) – can

evolve into a stable small amplitude pattern. In other words, the nonlinear spatial effects destabilize all 'natural' small amplitude spatially periodic patterns – *even in the supercritical case.* (In fact, the situation is even slightly worse, since there are two additional regions in the (a, b) plane within which neither of the waves described by (2.44) is stable – see [52].) In a way, this surprising mechanism only makes this pattern generating Hopf bifurcation more interesting: complex Ginzburg-Landau equation (2.42) has an extremely rich – and far from fully understood – structure of asymptotically stable solutions (that are more complex than the plane waves considered here), especially if $1 + ab < 0$ – see [2]. All of these correspond to stable small amplitude patterns in (1.2) (if μ is such that a Hopf bifurcation occurs in the reaction ODE (2.7)).

Proof of Lemma 2.7. The proof runs completely along the lines of that of the real case (Lemma 2.3). Thus, we introduce $B(\xi, \tau)$ by writing $A(\xi, \tau) = (R + B(\xi, \tau))e^{i(K\xi+W\tau)}$, linearize and decompose $B(\xi, \tau)$ into $U(\xi, \tau)) + iV(\xi, \tau)$, set $(U(\xi, \tau), V(\xi, \tau)) = (\alpha, \beta)e^{ik\xi+\lambda\tau}$ with $k \in \mathbb{R}$ and $\lambda = \lambda(k) \in \mathbb{C}$ (cf. (2.1)) and obtain,

$$\begin{pmatrix} -2R^2 - k^2 - 2iaKk & +ak^2 - 2iKk \\ -2bR^2 - ak^2 + 2iKk & -k^2 - 2iaKk \end{pmatrix} \begin{pmatrix} \alpha \\ \beta \end{pmatrix} = \lambda \begin{pmatrix} \alpha \\ \beta \end{pmatrix},$$

the complex counterpart of (2.39). Expanding the solutions $\lambda_{1,2}(k) \in \mathbb{C}$ of the associated characteristic equation in k – recall that $|k| \ll 1$ for the sideband instability – yields,

$$\mathrm{Re}\,(\lambda_1)\,(k) = -2R^2 + \mathcal{O}(k^2), \;\; \mathrm{Re}\,(\lambda_2)\,(k) = -\left((1 + ab) - 2(1 + b^2)\frac{K^2}{R^2}\right)k^2 + \mathcal{O}(k^4), \tag{2.45}$$

from which the Lemma follows. □

Remark 2.8 If λ_1 is not real at criticality – i.e. if $\lambda_1(k_c; \mu_c) \notin i\mathbb{R}$ – one typically needs to also redefine the spatial coordinate ξ into a travelling coordinate, $\xi = \varepsilon(x - c_g t)$ with $ic_g = -\frac{d\lambda_1}{dk}(0; \mu_c) \in i\mathbb{R}$ (cf. (2.13)), where c_g is called the *group velocity* of the 'package of unstable waves'. Due to the reversibility symmetry of (1.2) and the fact that $k_c = 0$ it follows that $c_g = 0$ here. However, nontrivial group velocities will appear in reaction-*advection*-diffusion systems in which an advection term breaks the reversibility – see for instance [85] – or in reaction-diffusion models with 3 or more components – see the upcoming subsection.

2.5.2 Other mechanisms

If reaction-diffusion system (1.1) has $N \geq 3$ components (section 5.1.2), and is defined on $\mathbb{R}$, then a Turing-Hopf bifurcation may take place – where we define a Turing-Hopf bifurcation as being associated to a linear destabilization at which the critical eigenvalue curve $\mathrm{Re}(\lambda_1(k; \mu))$ is tangent to the real axis at $(k, \mu) = (k_c, \mu_c)$ with $k_c \neq 0$ such that $\mathrm{Im}(\lambda_1(k_c; \mu_c)) \neq 0$. (Note that the name 'Turing-Hopf' is sometimes also used as generalized terminology for all types of 'oscillating' – spatial and/or temporal – pattern generating mechanisms discussed here [65, 85] – see Fig. 3(a).) As explained in section 2.1, this cannot happen with $N = 2$ in (1.2), but is certainly possible for $N \geq 3$. In that case, there are two critical waves, $E_{c,l}(x, t) = e^{i(k_c x+\omega_c t)}$ and $E_{c,r}(x, t) = e^{i(k_c x-\omega_c t)}$ with $i\omega_c = \lambda_1(k_c; \mu_c) \in i\mathbb{R}$. This leads to a coupled system of complex Ginzburg-Landau equations.

The final co-dimension 1 destabilization mechanism occurs when a real eigenvalue of the reaction ODE (2.7) crosses through zero: a transcritical bifurcation in the ODE that corresponds to a quadratic tangency at $k_c = 0$ of a real-valued $\lambda_1(k)$ at criticality (i.e. at $\mu = \mu_c$). In the PDE, a second trivial state $(\bar{U}_2, \bar{V}_2)$ passes through $(\bar{U}, \bar{V})$, while exchanging stability type. The associated modulation equation is real valued – i.e. $A(\xi, \tau) : \mathbb{R} \times \mathbb{R}^+ \to \mathbb{R}$ instead of $\mathbb{C}$ – and is of Fischer-KPP type (cf. (4.5)). This bifurcation only yields very simple patterns, however, there again is a very rich pattern generating structure at/near the co-dimension 2 point at which the Turing bifurcation merges with this bifurcation, i.e. when $k_c(\nu) \downarrow 0$ as function of a second parameter ν (as in the limit $\nu \to \sqrt{d}$ in (2.31) for the explicit example (2.30)). See [69] and the references therein.

3 Bridging the gap: spatially periodic patterns and the Busse balloon

We return to the most typical mechanism by which patterns are initiated in reaction-diffusion systems, the Turing bifurcation of Theorem 2.4. We ask the – natural – question, *What happens to these (small amplitude) Turing patterns as μ is no longer asymptotically close to μ_c?* This is in fact a *necessary* question: in reality a parameter is 'never' asymptotically close to a bifurcation value, thus we need to be able to vary μ away from μ_c.

However, before doing so, we also need to realize that there is an aspect of Theorem 2.4 we so far not discussed that is a priori remarkable: it establishes the existence of *a continuous family of stationary, spatially periodic patterns.* Moreover, these patterns are by construction *symmetric* – see Remark 3.2. A stationary pattern in (1.2) corresponds to a solution of the stationary ODE associated to (1.2) that is obtained by setting $(U(x,t), V(x,t)) = (u(x), v(x))$,

$$\left\{ \begin{array}{rcrcl} u_{xx} & + & G(u,v;\mu) & = & 0, \\ dv_{xx} & + & H(u,v;\mu) & = & 0, \end{array} \right. \tag{3.1}$$

which can equivalently be written as a 4-dimensional spatial dynamical system in $(u(x), p(x), v(x), q(x))$ with $p(x) = u_x(x)$, $q(x) = \sqrt{d}v_x(x)$,

$$\left\{ \begin{array}{rcl} u_x & = & p \\ p_x & = & -G(u,v;\mu) \\ v_x & = & \frac{1}{\sqrt{d}}q \\ q_x & = & -\frac{1}{\sqrt{d}}H(u,v;\mu) \end{array} \right. \tag{3.2}$$

A stationary spatially periodic pattern of (1.2) corresponds to a periodic solution $\gamma_{\rm p}(x)$ of (3.2), i.e. to a closed orbit in the 4-dimensional phase space associated to (3.2). In contrast to the statement of Theorem 2.4, it seems a priori 'unlikely' that such a closed orbit could be embedded in a continuous family of similar orbits. In general, this is certainly also not the case. Here, it is a consequence of the $x \to -x$ symmetry of reaction-diffusion systems (1.1)/(1.2) – as we shall show in the upcoming section. Although (1.1)/(1.2) certainly also exhibit non-symmetric patterns – in fact, uniformly traveling patterns cannot be symmetric – we will for simplicity – and to give a flavor of the main ideas – only consider symmetric, stationary patterns in this section (as well as in the next section).

3.1 Symmetric spatially periodic patterns

In the 4-dimensional setting of (3.2), the $x \to -x$ symmetry of (1.2) corresponds to the *reversibility symmetry*,

$$\mathcal{R}\left(u(x), p(x), v(x), q(x)\right) = (u(-x), -p(-x), v(-x), -q(-x)). \tag{3.3}$$

The (stationary) symmetric solutions of (1.2) considered here are solutions $\gamma(x)$ of (3.2) that satisfy $\mathcal{R}\left(\gamma(x)\right) \equiv \gamma(x)$. Note that we implicitly – and artificially (since one can always introduce a spatial translation) – have chosen $x = 0$ as point of symmetry. Note also that a symmetric solution must have $p(0) = q(0) = 0$, in other words, that $\gamma(x)$ intersects the plane $\{p = q = 0\}$ at $x = 0$ (and that all orbits intersecting $\{p = q = 0\}$ do so in a transversal way, since $(u_x, p_x, v_x, q_x) = (0, -G(u,v), 0, -H(u,v)/\sqrt{d})$ at the intersection).

In this section – and in section 4.1.2 – we present some generic results on the existence of stationary symmetric patterns in the 2-component system (1.2), i.e. on existence problem (3.2). Our arguments are essentially geometrical and our statements can be generalized to N-component models or be extended to travelling heteroclinic fronts and to travelling spatially periodic patterns – called 'wave trains'. (In this analysis, the free parameter c – the speed – takes over the role of the symmetry $\mathcal{R}$ – see also Remark 4.13.) Nevertheless, we keep simplicity as our guiding principle and focus on symmetric solutions.

Let's assume that we know that $\gamma_{\rm p}(x) = (u_{\rm p}(x), p_{\rm p}(x), v_{\rm p}(x), q_{\rm p}(x))$ is a symmetric periodic solution of

(3.2) with (minimal) period $T > 0$. By defining y as a shift of x over $T/2$, we notice by (3.3) that,

$$\begin{array}{rcl} \gamma_{\rm p}(y) & = & (u_{\rm p}(\frac{1}{2}T+y), p_{\rm p}(\frac{1}{2}T+y), v_{\rm p}(\frac{1}{2}T+y), q_{\rm p}(\frac{1}{2}T+y)) \\ & = & (u_{\rm p}(-\frac{1}{2}T+y), p_{\rm p}(-\frac{1}{2}T+y), v_{\rm p}(-\frac{1}{2}T+y), q_{\rm p}(-\frac{1}{2}T+y)) \\ & = & (u_{\rm p}(\frac{1}{2}T-y), -p_{\rm p}(\frac{1}{2}T-y), v_{\rm p}(\frac{1}{2}T-y), -q_{\rm p}(\frac{1}{2}T-y)) \\ & = & \mathcal{R}\left(\gamma_{\rm p}(y)\right), \end{array} \tag{3.4}$$

which implies that $\gamma_{\rm p}(x)$ is not only symmetric in the $\{p = q = 0\}$ plane at $x = 0$ (and at all $x = kT$, $k \in \mathbb{Z}\mathbb{Z}$), but also exactly halfway through each period, i.e. at $x = T/2 + lT$, $l \in \mathbb{Z}\mathbb{Z}$. In other words, the closed curve (in phase space) associated to $\gamma_{\rm p}(x)$ intersects $\{p = q = 0\}$ twice (transversally) and is symmetric in $\{p = q = 0\}$. It now follows that $\gamma_{\rm p}(x)$ must be embedded in a 1-parameter family.

Lemma 3.1 *Let $\gamma_{\rm p}(x;\mu_0)$ be a symmetric periodic solution of (3.2), then (3.2) must have a 1-parameter family of periodic solutions $\gamma_{{\rm p},\sigma}(x;\mu)$ for $\sigma \in \Sigma \subset \mathbb{R}$ open (and $\gamma_{\rm p}(x;\mu_0) = \gamma_{{\rm p},\sigma_0}(x;\mu_0)$ for certain $\sigma_0 \in \Sigma$). Moreover, this family persists as μ is varied around μ_0.*

Thus, the existence of a symmetric periodic solution $\gamma_{\rm p}(x)$ of (3.2) for a certain parameter μ_0, implies the existence of 1-parameter families of such solutions for each μ in an open neighborhood of μ_0. Moreover, the stationary small amplitude spatially periodic patterns generated by the supercritical Turing bifurcation of Theorem 2.4 are of the type described by this Lemma (Remark 3.2) and these can thus be extended 'beyond onset', i.e. beyond the asymptotically small validity region of Theorem 2.4. (We refer to [39] for a detailed discussion of the bifurcating periodic Turing orbits as generated by the associate reversible 1 : 1 Hopf bifurcation in (3.2) – see also section 4.1.1.)

Proof. Consider a sufficiently small open neighborhood $\mathcal{V}_{\rm p} \subset \{p = q = 0\}$ of one of the intersections of $\gamma_{\rm p}(x;\mu)$ with $\{p = q = 0\}$ – say $x = 0$ – and define the '3-dimensional strip' $\S_{\rm p}^+ \subset \mathbb{R}^4$ as the set spanned by the solutions $\phi(x)$ of (3.2) that have $\phi(0) \in \mathcal{V}_{\rm p}$. Clearly, after a half a loop, $\S_{\rm p}^+$ must intersect $\{p = q = 0\}$ again near $\gamma_{\rm p}(T/2;\mu_0) \in \{p = q = 0\}$ (3.4). Since $\gamma_{\rm p}(x;\mu)$ intersects $\{p = q = 0\}$ transversally, this intersection of (3-dimensional) $\S_{\rm p}^+$ with (2-dimensional) $\{p = q = 0\}$ must be a 1-dimensional curve $m_{\rm p}^1 \ni \gamma_{\rm p}(T/2;\mu_0)$. By flowing backwards, we know that there is another 1-dimensional curve $m_{\rm p}^0 \subset \mathcal{V}_{\rm p} \subset \{p = q = 0\}$ – with $\gamma_{\rm p}(0;\mu_0) \in m_{\rm p}^0$ – such that orbits through $Q_\sigma \in m_{\rm p}^0$ intersect $\{p = q = 0\}$ in $m_{\rm p}^1$. The symmetry (3.3) implies that each of these orbits is a symmetric periodic orbit $\gamma_{{\rm p},\sigma}(x;\mu)$. This structure is robust under (small) variations of μ. □

Remark 3.2 Imposing the $x \to -x$ symmetry on Ansatz (2.20) implies that Ginzburg-Landau equation (2.29) must be symmetric with respect to $A(\xi,\tau) \to \bar{A}(\xi,\tau)$ – *in the case of reversible patterns.* In other words, $\bar{A}(\xi,\tau)$ must be a solution of (2.29) if $A(\xi,\tau)$ is. Hence, a Ginzburg-Landau equation describing reversible patterns must have *real coefficients* – as is the case for (2.29) – and vice versa. Note that this is not the case for (2.42): the Hopf bifurcation of section 2.5.1 generates non-symmetric patterns.

3.2 The Busse balloon

In [6], Friedrich Busse determined – by numerical simulations – a region in (Rayleigh number R, wave number k)-space for which a fluid heated from below exhibits stable convective 'roll patterns' – the Rayleigh number R is a (scaled) parameter that is proportional to the temperature difference driving the flow. This region became knows as 'the Busse balloon' and it has been playing a crucial role in understanding the transition from the stationary purely conductive state to the turbulent state that takes place as the R is increased. Of course this concept is not restricted to hydrodynamical stability problems.

Definition 3.3 *A* **Busse balloon** *associated to reaction-diffusion system (1.1)/(1.2) with parameter μ is a set $\mathbf{B} \subset$ (parameter μ, wave number k)-space, such that any $(\mu_0, k_0) \in \mathbf{B}$ corresponds to a stable spatially periodic solution of (1.1)/(1.2) at $\mu = \mu_0$ with wave number $k = k_0$.*

The Turing bifurcation established by Theorem 2.4 provides a leading order description of the 'nose' of a Busse balloon: at one side of μ_c, i.e. for $\tilde{\mu}$ such that $\tilde{\mu}\lambda_\mu^c < 0$, there are no stable spatially periodic

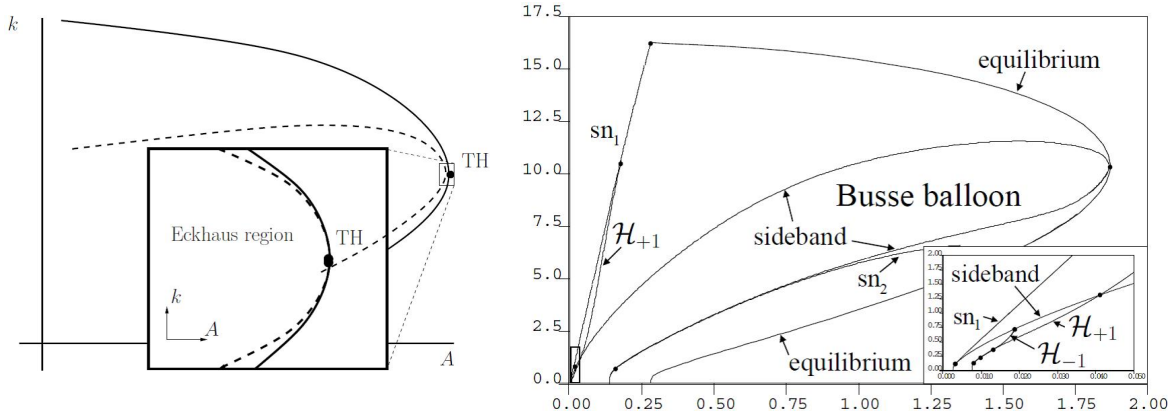

Figure 3: (a) From [85]: the approximation of the 'nose' of the Busse balloon by Eckhaus parabola (3.5) (dashed line); the continuous line indicates the boundary of the associated existence balloon. (b) From [24]: a Busse balloon for the Gray-Scott model in (parameter A, wave number k)-space embedded in an existence balloon.

patterns, while a continuous band of such patterns is created as $\tilde{\mu}\lambda_\mu^c$ increases through 0. In fact, it follows from Theorem 2.4 – more precisely by setting $K = \pm 1/\sqrt{3}$ in (2.41) – that the boundary of this region and thus *the boundary of the Busse balloon* is at leading order described by the *Eckhaus parabola*,

$$\mu_{\mathrm{E}}(k) = \mu_c + \frac{3|\lambda_{k^2}^c|}{2\lambda_\mu^c}(k-k_c)^2 \ \text{ with } \ k - k_c = \mathcal{O}(\varepsilon), \tag{3.5}$$

that gives a (leading order) description of the 'Eckhaus nose' of the associated Busse balloon – see Fig. 3(a). The Busse balloon is embedded in an *existence balloon*, i.e. a region in (parameter, wave number k)-space for which (1.2) has (stable or unstable) spatially periodic patterns, whose 'nose' is also described by Theorem 2.4 (and is at leading order described by setting $K = \pm 1$ in (2.41)) – see Fig. 3(a). Now we know from Lemma 3.1 that the existence balloon can be extended beyond the asymptotically small region near the Turing bifurcation. The Busse balloon is defined as the 'sub-balloon' of stable patterns, it can be determined numerically by means of continuation techniques – see especially [66].

In Fig. 3(b) a (numerical plot of a) Busse balloon for the Gray-Scott model is presented in (parameter A, wave number k)-space (and $B = 0.26$, $d = 0.001$ fixed – see Fig. 1). Surprisingly little is known about the general nature of the Busse balloon, especially of its boundary and of the *bifurcations* periodic patterns undergo as parameters cross through the boundary. However, in [65] the types of all robust co-dimension 1 *destabilizations* of (stationary, reversible) Turing patterns as considered here is established: pure Turing, pure Hopf, Turing-Hopf, period doubling (see Fig. 5(a)), sideband, and saddle node or pitchfork. We refrain from giving detailed descriptions of these mechanisms and refer to [65]. However, we note that the Eckhaus nose of sideband destabilizations of Theorem 2.4 and Lemma 2.3 extends way beyond the Turing bifurcation in the Busse balloon of Fig. 3(b), only as wave number k gets small – i.e. when the patterns are of the type given in Fig. 4(c) – it's taken over by a curve of saddle node bifurcations on the lower branch, and by Hopf destabilizations on the upper branch – see especially the inset in Fig. 3(b). Both these 'new' boundaries have intriguing – not fully understood – consequences. The saddle node curve represents the onset of the pulse self-replication mechanism the Gray-Scott model is famous for [22, 51, 67] and the intersection of the Hopf curve is the first of countably many intersections – and thus co-dimension 2 points – accumulating on the 'homoclinic tip' at the extreme left hand side of the Busse balloon at/near $k = 0$, i.e. at/near the homoclinic limit where $T \to \infty$, with $T =$ the period of the (stable) spatially periodic patterns, see [23, 24].

Clearly, the Gray-Scott Busse balloon of Fig. 3(b) bridges the gap between the small amplitude patterns at the Eckhaus nose of section 2 – where the first stable periodic patterns are created by the Turing bifurcation – and the 'far from equilibrium' localized structures of upcoming section 4 – where the '$T = \infty$' homoclinic orbit of Fig. 4(a) is the last spatially periodic pattern to destabilize. It certainly is not necessary that a Busse balloon that 'opens' with a Turing bifurcation must 'close' with a homoclinic tip – see for instance [38] for an (ecological) example of pattern formation between 2 different types of Turing bifurcations. However, the Busse balloon of Fig. 3(b) appears to be representative for a large class of

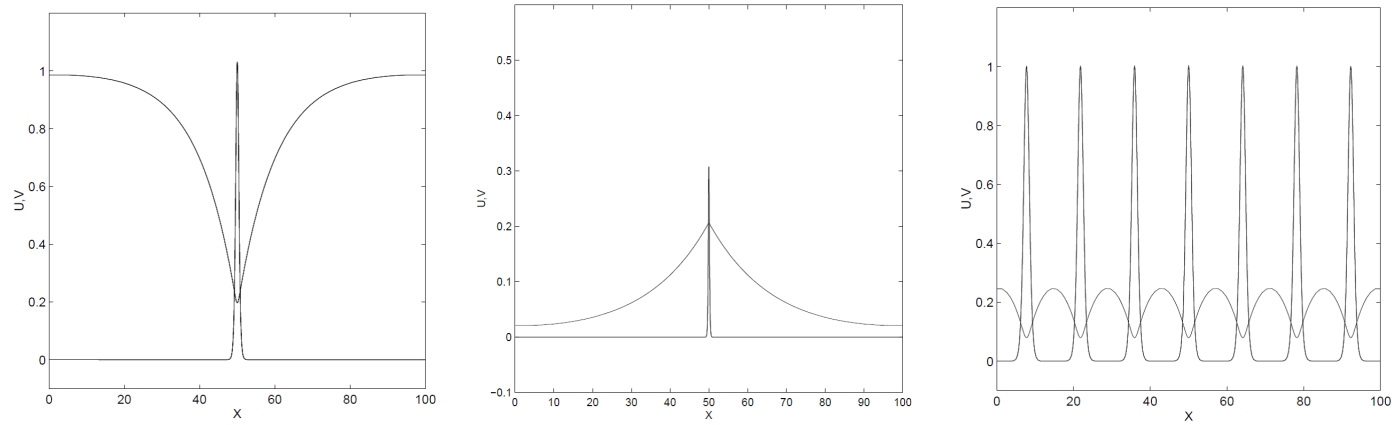

Figure 4: Stable symmetric, homoclinic pulse patterns in the Gray-Scott (a) and Gierer-Meinhardt (b) models [17, 18]. (c) A typical 'far from equilibrium' spatially periodic multi-pulse pattern in the Gray-Scott model (that appears for (parameter A, wave number k)-values near the 'homoclinic tip' of the Busse balloon of Fig. 3(b).

reaction-diffusion systems: all Busse balloons in [74, 76, 77, 85] have the 'bridging the gap'-structure between Eckhaus nose and homoclinic tip of Fig. 3(b). In Lemma 4.5 of section 4.1.2 we show that homoclinic orbits indeed typically appear as 'end points' of the families of periodic solutions of Lemma 3.1. A priori, this existence result does not imply that a Busse balloon should 'close' with such a homoclinic pattern. However, in [60] it was claimed that '*the homoclinic pattern is the last to become unstable*' in the generalized Gierer-Meinhardt model [36]. This conjecture has been shown to hold in a large class of 2-component reaction-diffusion models [23, 24]. Therefore, the Busse balloon can indeed be considered as crucial – but certainly not yet well-studied – *bridging concept* between the classical Turing patterns *near onset* and localized *far from equilibrium* patterns.

4 Far from equilibrium: localized structures

In general a 'localized structure' is a solution of (1.1)/(1.2) that is 'close' to one or more 'background' states $(\bar{U}, \bar{V})$ for almost all $x \in \mathbb{R}$, except for one or more 'intervals' in which it diverges away from these. The simplest localized structures are stationary solutions, or solutions that are stationary in a frame that travels with a constant speed c. Here, we focus on *symmetric* stationary localized solutions of 2-component model (1.2), partly for reasons of transparency of presentation, but mostly since we saw in section 3 – especially in Fig. 3(b) – that these patterns turn up naturally as 'end products' of the Turing bifurcations of section 2. These patterns correspond to symmetric *homoclinic* orbits in (3.2), i.e. solutions $\gamma_{\rm h}(x)$ of (3.2) that approach the same critical point $\bar{P}$ as $x \to \pm\infty$. It is thus crucial to understand the local character of the critical points $\bar{P} = (\bar{U}, 0, \bar{V}, 0)$ of (3.2).

4.1 Some a priori observations

4.1.1 Relations between $(\bar{U}, \bar{V})$ and $(\bar{U}, 0, \bar{V}, 0)$ as critical points of (2.7) and (3.2)

In the scalar case – $N = n = 1$ in (1.1) – there is a direct, somewhat counterintuitive, relation between the character of the critical points $u(t) \equiv \bar{U}$ and $(u(x), p(x)) \equiv (\bar{U}, 0)$ of the scalar counterparts of reaction ODE (2.7) – $\dot{u} = F(u; \mu)$ – and spatial system (3.2) –

$$u_{xx} + F(u; \mu) = 0, \quad \text{or} \quad \left\{ \begin{array}{rcl} u_x & = & p \\ p_x & = & -F(u; \mu) \end{array} \right. \tag{4.1}$$

Clearly, $\bar{U}$ is stable as solution of the reaction ODE if $f_u = \frac{dF}{dU}(\bar{U}; \mu) < 0$. In fact, in this case $\bar{U}$ is linearly stable as solution of the scalar PDE on $\mathbb{R}$ – it follows by (2.1) that $\lambda(k; \mu) = f_u - k^2 < 0$, $k \in \mathbb{R}$. Note that this also implies – confirms – that a Turing bifurcation is impossible in scalar equations: $\bar{U}$ can only be unstable in (1.1) if it is already unstable in the reaction ODE. The stability condition $f_u < 0$ implies

that $(\bar{U},0)$ is a saddle in existence system (4.1) – with eigenvalues $\Lambda_{1,2}=\pm\sqrt{-f_u}$; if $(\bar{U},0)$ is a center, i.e. if $f_u>0$ and $\Lambda_{1,2}=\pm i\sqrt{f_u}$, then $\bar{U}$ is unstable as solution of (1.1) on $\mathbb{R}$.

Lemma 4.1 *Let $U(x,t)\equiv\bar{U}$ be a trivial solution of (1.1) with $N=n=1$ and let $(\bar{U},0)$ be the associated critical point of spatial system (4.1). Then $\bar{U}$ is spectrally stable, respectively unstable, as solution of (1.1) on $\mathbb{R}$ if the critical point $(\bar{U},0)$ of (4.1) is a saddle, resp. a center – and vice versa.*

In the 2-component case, similar relations may be deduced, however, these are less transparent and more involved. The local character of $\bar{P}=(\bar{U},0,\bar{V},0)$ is determined by the 4×4 matrix,

$$\mathcal{B}(\mu)=\begin{pmatrix} 0 & 1 & 0 & 0\\ -g_u & 0 & -g_v & 0\\ 0 & 0 & 0 & \frac{1}{\sqrt{d}}\\ -\frac{1}{\sqrt{d}}h_u & 0 & -\frac{1}{\sqrt{d}}h_v & 0\end{pmatrix}, \tag{4.2}$$

with g_u etc. as in (2.3) and with characteristic equation,

$$\Lambda^4+\frac{1}{d}(dg_u+h_v)\Lambda^2+\frac{1}{d}(g_uh_v-g_vh_u)=0, \tag{4.3}$$

for 'spatial' eigenvalues $\Lambda_j=\Lambda_j(\mu)$, $j=1,...,4$. Note that this is a quadratic equation in $\ell=\Lambda^2$ – induced by symmetry (3.3). Note also that we can identify the Turing bifurcation of section 2 by observing that (2.10) is equivalent to the condition that the 2 solutions $\ell_\pm$ of (4.3) – in ℓ – merge. This implies by (2.5) that at the Turing bifurcation, matrix $\mathcal{B}(\mu_c)$ has a pair purely imaginary eigenvalues of multiplicity 2, $\Lambda_{1,2}(\mu_c)=+i\sqrt{(dg_u+h_v)/2d}$, $\Lambda_{3,4}(\mu_c)=-i\sqrt{(dg_u+h_v)/2d}$. It is straightforward to check that $\Lambda_{1,2}(\mu)$ splits into a pair of purely imaginary eigenvalues as $(\bar{U},\bar{V})$ becomes unstable in (1.2) by the Turing destabilization of Lemma 2.1 (with still $\Lambda_{3,4}(\mu)=-\Lambda_{1,2}(\mu)\in i\mathbb{R}$), and that all 4 eigenvalues are away from the imaginary axis before the destabilization (so that $\Lambda_1(\mu)=-\Lambda_2(\mu)=\bar{\Lambda}_3(\mu)=-\bar{\Lambda}_4(\mu)$): a Turing bifurcation in (1.2) corresponds to a reversible $1:1$ Hopf bifurcation in spatial problem (3.2) – see [39].

As in the scalar case, there is a direct relation between instability of $(\bar{U},\bar{V})$ as solution of (1.2) and having a pair of purely imaginary eigenvalues in spatial problem (3.2) (i.e. having a solution $\ell=\Lambda^2<0$ of (4.3)). This is because such a pair of eigenvalues corresponds to a value k_i of k such that the characteristic polynominal (2.4) associated to the stability of $(\bar{U},\bar{V})$ as solution of (1.2) on $\mathbb{R}$ has a temporal eigenvalue $\lambda(k)=0$ at $k=\pm k_i$: the perturbation in (2.1) is stationary at $\lambda(\pm k_i)=0$, which builds a natural bridge from the temporal stability problem for $(\bar{U},\bar{V})$ in (1.2) to the character of $\bar{P}$ in system (3.2). This equivalence is confirmed by checking that if (α_i,β_i) is an eigenvector of $\mathcal{A}(k_i;\mu)$ (2.2) associated to $\lambda(k_i)=0$, then $(\alpha_i,ik_i\alpha_i,\beta_i,ik_i\sqrt{d}\beta_i)$ is an eigenvector of $\mathcal{B}(\mu)$ (4.2) with eigenvalue $\Lambda=ik_i$ (and vice versa). It follows that there must be values $k>k_i$, or $k<k_i$, for which $\lambda(k)>0$, which indeed implies that $(\bar{U},\bar{V})$ is unstable. See section 4.3.2 for a further interpretation of the relation between the temporal and spatial eigenvalue problems (2.4) and (4.3).

Since we are interested in localized structures that correspond to homoclinic connections to a critical point $\bar{P}$ of (3.2), we are interested in the stable and unstable manifolds $W^s(\bar{P})$ and $W^u(\bar{P})$ of $\bar{P}$: a homoclinic solution must lie in the intersection $W^s(\bar{P})\cap W^u(\bar{P})$. The above relation between zeroes of solutions $\lambda(k)$ of (2.4) and spatial eigenvalues $\Lambda\in i\mathbb{R}$ of (4.2) implies that $(\bar{U},\bar{V})$ must be unstable as solution (1.2) on $\mathbb{R}$ if $\dim\big(W^{s,u}(\bar{P})\big)<2$. This yields a simple observation that is useful for the construction of pulse patterns that connect end states that are stable as solutions of (1.2) on $\mathbb{R}$.

Lemma 4.2 *Let $\bar{P}=(\bar{U},0,\bar{V},0)$ be a critical point of (3.2) that corresponds to a stable trivial state $(\bar{U},\bar{V})$ of (1.2) on $\mathbb{R}$, then $\dim\big(W^s(\bar{P})\big)=\dim\big(W^u(\bar{P})\big)=2$: $\bar{P}$ is a saddle point of (3.2).*

The reverse is in general not true. A critical point that has $\dim(W^s(\bar{P}))=\dim(W^u(\bar{P}))=2$ does not necessarily correspond to a stable trivial state in (1.2), since the critical solution $\lambda_1(k)$ of (2.4) does not have to enter the unstable half plane by crossing through $\lambda=0$ – which would imply that $\bar{P}$ must have a center direction (and thus that $\dim\big(W^{s,u}(\bar{P})\big)<2$); $\lambda_1(k)$ may also cross through $\mathrm{Re}(\lambda)=0$ with $\mathrm{Im}(\lambda_1)\neq 0$. Such a crossing – with associated destabilization of $(\bar{U},\bar{V})$ – does not have a direct interpretation in terms of the (spatial) eigenvalues of $\mathcal{B}(\mu)$. This can – for instance – be checked more explicitly by determining

the spatial eigenvalues Λ_j of a critical point $\bar{P}$ that is associated to a pattern $(\bar{U},\bar{V})$ in (1.2) that is near a Hopf bifurcation – see section 2.5.1, Fig. 2(c). In such a case, $g_u + h_v$ is small and $g_u h_v - g_v h_u > 0$, and a straightforward analysis of (4.2) with g_u passing through $-h_v$ shows that a saddle $\bar{P}$ – thus with $\dim\big(W^s(\bar{P})\big) = \dim\big(W^u(\bar{P})\big) = 2$ – can correspond to both a stable or an unstable trivial pattern in (1.2) (either with $\Lambda_j \in \mathbb{R}$ $(j = 1, ..., 4)$ or $\Lambda_j \notin \mathbb{R}$ $(j = 1, ..., 4)$). However, with one additional – natural – assumption, it is possible to establish a relation between saddle points in (3.2) and stability in the PDE.

Lemma 4.3 *If* $\dim\big(W^s(\bar{P})\big) = \dim\big(W^u(\bar{P})\big) = 2$ *and* $(\bar{U},\bar{V})$ *is stable as solution of the reaction ODE (2.7), then* $(\bar{U},\bar{V})$ *is stable as solution of (1.2) on* $\mathbb{R}$.

Proof. Assume $(\bar{U},\bar{V})$ is unstable as solution (1.2), i.e. that there are positive k-values such that the solution $\lambda_1(k)$ of the characteristic polynomial (2.4) has $\mathrm{Re}(\lambda_1(k)) > 0$. Since $\lambda_1(k)$ must become negative for k sufficiently large (section 2.1) and $\mathrm{Re}(\lambda_1(0)) < 0$ – $(\bar{U},\bar{V})$ is stable in (2.7) – $\mathrm{Re}(\lambda_1(k))$ must cross twice through 0 as k increases from 0 to ∞. This cannot happen for $\lambda_1(k) \notin \mathbb{R}$ by (2.6): $\lambda_1(k)$ must be real at both crossings, which yields that $\dim\big(W^{s,u}(\bar{P})\big) = 0$. $\square$.

4.1.2 Generic properties of symmetric homoclinic solutions

Similar to the approach of section 3.1, we now assume we know that for a certain value μ_h of μ, (3.2) has a symmetric homoclinic solution $\gamma_\mathrm{h}(x;\mu_\mathrm{h}) = (u_\mathrm{h}(x;\mu_\mathrm{h}), p_\mathrm{h}(x;\mu_\mathrm{h}), v_\mathrm{h}(x;\mu_\mathrm{h}), q_\mathrm{h}(x;\mu_\mathrm{h}))$ – thus with $\gamma_\mathrm{h}(0;\mu_\mathrm{h}) = (u_\mathrm{h}(0;\mu_\mathrm{h}), 0, v_\mathrm{h}(0;\mu_\mathrm{h}), 0)) \in \{p = q = 0\}$ – that is homoclinic to a critical point $\bar{P} = \bar{P}(\mu_\mathrm{h})$ that corresponds to a stable state $(\bar{U},\bar{V})$ of (1.2) on $\mathbb{R}$. We also assume that $\gamma_\mathrm{h}(x;\mu_\mathrm{h})$ is a *non-degenerate* symmetric homoclinic orbit, in the sense that the 2-dimensional manifolds $W^s(\bar{P}(\mu_\mathrm{h}))$ and $W^u(\bar{P}(\mu_\mathrm{h}))$ – Lemma 4.2 – intersect in a transversal way, i.e. that they are not tangent along their intersection $W^s(\bar{P}(\mu_\mathrm{h})) \cap W^u(\bar{P}(\mu_\mathrm{h})) \supset \gamma_\mathrm{h}(x;\mu_\mathrm{h})$. Then, it follows that there is an open region in parameter space for which (3.2) has symmetric homoclinic orbits.

Lemma 4.4 *Let* $\gamma_\mathrm{h}(x;\mu_\mathrm{h})$ *be a non-degenerate symmetric homoclinic solution of (3.2) (in the sense of the preceding formulation), then there is an open neighborhood* Ω_h *of* μ_h *(in parameter space) such that (3.2) has a non-degenerate symmetric homoclinic solution* $\gamma_\mathrm{h}(x;\mu)$ *to the critical point* $\bar{P}(\mu)$ *for all* $\mu \in \Omega_\mathrm{h}$.

Thus, although we know by Lemma 4.2 that $\dim\big(W^s(\bar{P})\big) + \dim\big(W^u(\bar{P})\big) = 4 =$ the dimension of the phase space of (3.2), and one would expect that one needs to 'tune' a parameter to have a 1-dimensional intersection $W^s(\bar{P}) \cap W^u(\bar{P})$, symmetry (3.3) warrants that this is not the case: symmetric homoclinic solutions appear in open parameter regions.

Proof. We define the curve $\ell^s(\mu_\mathrm{h})$ as the 1-dimensional intersection of $W^s(\bar{P}(\mu_\mathrm{h}))$ with the 3-dimensional plane $\{p = 0\}$ ($\dim(\ell^s(\mu_\mathrm{h})) = 1$, since dim(phase space) = 4). It follows from the assumption that symmetric orbit $\gamma_\mathrm{h}(x;\mu_\mathrm{h})$ exists that $\ell^s(\mu_\mathrm{h})$ intersects the 2-dimensional subplane $\{q = 0\}$ – i.e. $\{p = q = 0\}$. By (3.3), the curve $\ell^u(\mu_\mathrm{h}) = W^u(\bar{P}(\mu_\mathrm{h})) \cap \{p = 0\}$ is the symmetrical counterpart of $\ell^s(\mu_\mathrm{h})$ within the $\{q = 0\}$ plane ($\subset \{p = 0\}$), moreover, $\ell^s(\mu_\mathrm{h}) \cap \ell^u(\mu_\mathrm{h}) = \gamma_\mathrm{h}(0;\mu_\mathrm{h}) \in \{p = q = 0\}$. The assumption that $W^s(\bar{P}(\mu_\mathrm{h}))$ and $W^u(\bar{P}(\mu_\mathrm{h}))$ intersect transversally implies that (the curves) $\ell^s(\mu_\mathrm{h})$ and $\ell^s(\mu_\mathrm{h})$ must intersect (the plane) $\{q = 0\}$ transversally: if $\ell^s(\mu_\mathrm{h})$ would be tangent to $\{q = 0\}$ at the intersection $\ell^s(\mu_\mathrm{h}) \cap \{q = 0\}$, then – by symmetry – $\ell^s(\mu_\mathrm{h})$ would be tangent to $\ell^u(\mu_\mathrm{h})$ at $\ell^s(\mu_\mathrm{h}) \cap \ell^u(\mu_\mathrm{h})$.

Now consider μ sufficiently close to μ_h, it follows from smooth dependence of parameters in system (3.2) and the transversality of the intersection at $\mu = \mu_\mathrm{h}$, that $\ell^s(\mu) = W^s(\bar{P}(\mu)) \cap \{p = 0\}$ also intersects $\{q = 0\}$ transversally. Hence, $W^s(\bar{P}(\mu))$ intersects $\{p = q = 0\}$, which implies the existence of symmetric orbit $\gamma_\mathrm{h}(x;\mu) \subset W^s(\bar{P}(\mu)) \cap W^u(\bar{P}(\mu))$ (with $W^s(\bar{P}(\mu)) \cap W^u(\bar{P}(\mu)) \cap \{p = q = 0\} = \gamma_\mathrm{h}(0;\mu)$). $\square$

We can now also provide a justification of the observations in section 3.2 of 'homoclinic tips' of Busse balloons associated to (1.2) – Fig. 3(b) – at least, at the level of the existence problem: a family of spatially periodic solutions – Lemma 3.1 – can have a homoclinic, ∞-period limit, orbit as 'endpoint'.

Lemma 4.5 *Let* $\gamma_\mathrm{h}(x;\mu)$ *be as in as in Lemma 4.4, a symmetric non-degenerate homoclinic solution of (3.2) to a critical point* $\bar{P}$ *that corresponds to a stable pattern of (1.2). There is a family of symmetric periodic solutions* $\gamma_{\mathrm{p},\sigma}(x;\mu)$ *– with period* $T(\sigma)$ *for* $\sigma \in$ *a certain set* Σ *– that limits on* $\gamma_\mathrm{h}(x;\mu)$*: there is a* $\sigma^* \in \partial\Sigma$ *such that the closed orbits associated to* $\gamma_{\mathrm{p},\sigma}(x;\mu)$ *merge with the homoclinic structure spanned by* $\gamma_\mathrm{h}(x;\mu)$ *(in phase space) as* $\sigma \to \sigma^*$*; moreover,* $T(\sigma) \to \infty$ *as* $\sigma \to \sigma^*$.

Proof. As in the proof of Lemma 3.1, consider an open neighborhood $\mathcal{V}_{\rm h} \subset \{p = q = 0\}$ of 'the middle' $\gamma_{\rm h}(0;\mu)$ of symmetric homoclinic orbit $\gamma_{\rm h}(x;\mu)$ and define the 3-dimensional strip $\S_{\rm h}^+$ as the set spanned by solutions $\phi(x)$ of (3.2) with $\phi(0) \in \mathcal{V}_{\rm h}$. By taking $\mathcal{V}_{\rm h}$ sufficiently small we may assume that the orbits $\phi(x)$ – that follow $\gamma_{\rm h}(x;\mu)$ – enter a (sufficiently small, 4-dimensional) neighborhood $\mathcal{U}_{\bar{P}}$ of saddle $\bar{P}$ (Lemma 4.2) in which the flow of (3.2) is (at leading order) described by its linearization around $\bar{P}$. Since $\gamma_{\rm h}(x;\mu)$ is non-degenerate, we know that the curves $\ell^{s,u}(\mu) = W^{s,u}(\bar{P}(\mu)) \cup \{p = 0\}$ as defined in the proof of Lemma 4.4 intersect $\{p = q = 0\}$ – and thus $\mathcal{V}_{\rm h}$ – transversally. Thus, after passing along $\bar{P}$, $\S_{\rm h}^+$ splits up into two diverging sub-strips that follow opposite branches of the unstable manifold $W^u(\bar{P}(\mu))$ of $\bar{P}$ (in forward 'time' x). One of these again intersects $\{p = q = 0\}$ (near $\bar{P}$), the other cannot (Since this behavior is typical near saddle points, we refrain from going into the details of the flow $\subset \mathcal{U}_{\bar{P}}$.) Following the proof of Lemma 3.1, we denote the intersection $\S_{\rm h}^+ \cap \{p = q = 0\}$ by the (1-dimensional) curve $m_{\rm h,p}^1$. By construction, $m_{\rm h,p}^1$ has 'endpoint' $\bar{P}$ as boundary, it corresponds to the core $\gamma_{\rm h}(x;\mu)$ of strip $\S_{\rm h}^+$. (Note that if $\gamma_{\rm h}(x;\mu)$ is not non-degenerate, the symmetric curves $\ell^{s,u}(\mu)$ are tangent to each other, but also to $\mathcal{V}_{\rm h} \subset \{p = q = 0\}$ – see the proof of Lemma 4.4 – hence, $\S_{\rm h}^+$ does not split up as it passes along $\bar{P}$ and either or not intersects $\{p = q = 0\}$ – in the former case, $m_{\rm h,p}^1$ does not have $\bar{P}$ as 'endpoint' and passes through/extends beyond $\bar{P}$, in the latter case, $m_{\rm h,p}^1$ does not exist.)

As in the proof of Lemma 3.1, we define the 1-dimensional curve $m_{\rm h,p}^0 \subset \mathcal{V}_{\rm p} \subset \{p = q = 0\}$ – with $\gamma_{\rm h}(0;\mu) \in m_{\rm h,p}^0$ – such that solutions of (3.2) with initial values $Q_\sigma \in m_{\rm h,p}^0$ intersect $\{p = q = 0\} \cap \mathcal{U}_{\bar{P}}$ in $m_{\rm h,p}^1$. Once again, symmetry (3.3) implies these must be symmetric periodic orbits: orbits $\gamma_{{\rm p},\sigma}(x;\mu)$. The critical value σ^* corresponds to the limit $Q_\sigma \to \gamma_{\rm h}(0;\mu)$ – associated to the 'endpoint' $\bar{P}$ on $m_{\rm h,p}^1$ – in which $\gamma_{{\rm p},\sigma}(x;\mu)$ merges with homoclinic orbit $\gamma_{\rm h}(x;\mu)$. Hence, $T(\sigma) \to \infty$ as $\sigma \to \sigma^*$. □

4.2 The existence of stationary pulse solutions

4.2.1 The scalar problem

Although Lemma 4.4 provides good reasons to expect that symmetric homoclinic solutions may be found, it is absolutely not clear whether such orbits can also be constructed. As inspiration, we again first consider the scalar problem, i.e (1.1) with $N = n = 1$. Stationary localized structures correspond to homoclinic/heteroclinic orbits in spatial system (4.1). This equation is not only reversible, it is in fact an integrable 'nonlinear oscillator' with Hamiltonian,

$$H(u,p) = \frac{1}{2}p^2 + \mathcal{F}(u;\mu) \text{ with } \mathcal{F}(u;\mu) = \int_0^u F(\tilde{u};\mu)\, d\tilde{u}. \tag{4.4}$$

This is in general no longer the case in $N \geq 2$-component systems, i.e. (3.1) is not a (2 degree-of-freedom) Hamiltonian system. Saddles $(\bar{U}, 0)$ of (3.1) – the stable background states by Lemma 4.1 – typically (but certainly not necessarily) are connected to themselves by closed loops: symmetric homoclinic orbits occur quite naturally. This can be seen by sketching the phase portraits associated to the classical examples of the Nagumo and generalized Fischer-KPP equations,

$$(\text{N}) : U_t = U_{xx} + U(U-\mu)(1-U),\ 0 < \mu < 1, \quad (\text{gFKPP}) : U_t = U_{xx} - U + U^\mu,\ \mu > 1. \tag{4.5}$$

(note that the classical F-KPP equation corresponds to $\mu = 2$). There is a homoclinic orbit to $(0,0)$ in (4.5)-(N) for $0 < \mu < \frac{1}{2}$ and to $(1,0)$ for $\frac{1}{2} < \mu < 1$ (and two heteroclinic connections between $(0,0)$ and $(1,0)$ for $\mu = \frac{1}{2}$); there is a homoclinic solution to $(0,0)$ for all $\mu > 1$ in (4.5)-(gFKPP) – in fact, it is explicitly given by,

$$u_{\rm h}(x;\mu) = \left(\frac{\mu+1}{2\cosh^2 \frac{1}{2}(\mu-1)x} \right)^{\frac{1}{\mu-1}}. \tag{4.6}$$

Remark 4.6 It follows immediately from the integrable structure (4.4) of (4.1) that indeed periodic solutions occur in families and that every homoclinic orbit can be seen as the boundary of such a family of periodic solutions – thus confirming Lemmas 3.1 and 4.5 (for the scalar case $N = 1$).

4.2.2 The construction of symmetric homoclinic pulses in singularly perturbed systems

In general, there is no way to 'control' the stable and unstable manifolds $W^s(\bar{P})$ and $W^u(\bar{P})$ of a saddle point $\bar{P}$ of existence system (3.2) in such a way that they can be shown to intersect – i.e. that the existence of a (symmetric) homoclinic pulse solution $\gamma_{\rm h}(x) \subset W^s(\bar{P}) \cap W^u(\bar{P})$ of 4-dimensional system (3.2) can be established. However, such control is possible in the context of *singularly perturbed* systems. Since such systems also come up very naturally as models – for instance, scale separation is the driving mechanism behind pattern formation in ecosystems [68] – and since (by far) the largest part of the 'far from equilibrium' mathematical research on multi-component reaction-diffusion systems has been developed in the context of singularly perturbed systems – see [10, 28, 93] and the references therein – we restrict ourselves in this section to a singularly perturbed version of (1.2). Thus, we assume that $d = \varepsilon^2$ in (1.2), where ε is an asymptotically small parameter: $0 < \varepsilon \ll 1$. Note that this indeed implies that there is scale separation in (1.2): the *slow* $U(x,t)$ diffuses on a longer – *slower* – spatial scale than the (spatially) *fast* component $V(x,t)$ – see Fig. 1(b).

As in (2.30), we shift the background state $(\bar{U}, \bar{V})$ towards $(0,0)$ – i.e. we set $G(0,0) = H(0,0) = 0$ – and we split off the linear terms of $G(U,V)$ and $H(U,V)$,

$$G(U,V) = g_u U + g_v V + G_2(U,V;\varepsilon), \;\; H(U,V) = h_u U + h_v V + H_2(U,V;\varepsilon), \tag{4.7}$$

with g_u etc. as in (2.3). Note that we allow the nonlinear parts $G_2(U,V)/H_2(U,V)$ of $G(U,V)/H(U,V)$ to depend on ε and have suppressed their μ-dependence. For simplicity we set,

$$g_u = -\mu < 0, \; g_v = 0, \; h_u = 0, \; h_v = -\nu < 0. \tag{4.8}$$

This implies that $(0,0)$ is stable as critical point of the reaction ODE (2.7) and that $\bar{P} = (0,0,0,0)$ is saddle point in the existence ODE (3.2). It follows, either by Lemma 4.3 or by straightforward calculations, that $(0,0)$ is a stable background state of (1.2) on $\mathbb{R}$. Furthermore, we assume that the system is *slowly linear* [28], i.e. that the nonlinear terms only have impact in regions where fast component V is not 0,

$$G_2(U,0;\varepsilon) \equiv H_2(U,0;\varepsilon) \equiv 0, \; \frac{\partial G_2}{\partial V}(U,0;\varepsilon) \equiv \frac{\partial H_2}{\partial V}(U,0;\varepsilon) \equiv 0. \tag{4.9}$$

Finally, we assume that $H_2(U,V;\varepsilon)$ depends smoothly on ε, but that $G_2(U,V;\varepsilon)$ may be of $\mathcal{O}(1/\varepsilon)$,

$$G_2(U,V;\varepsilon) = \frac{\alpha(\varepsilon)}{\varepsilon}\, \tilde{G}_2(U,V;\varepsilon), \tag{4.10}$$

where $\alpha(\varepsilon)$ and $\tilde{G}_2(U,V;\varepsilon)$ are smooth in ε. Note that the a priori more natural case in which $G_2(U,V;\varepsilon)$ also varies smoothly in ε is included in (4.10) as the special situation $\alpha(\varepsilon) = \mathcal{O}(\varepsilon)$ – see also the 'validation' of (4.10) by Corollary 4.11. Together, these assumptions may seem to be too strong restrictions, but it should be noted that the literature on stationary localized structures in singularly perturbed reaction-diffusion systems has been largely developed in the context of the Gray-Scott and Gierer-Meinhardt models [36, 63] that satisfy the above assumptions. Moreover, the concept of *slowly nonlinear* reaction-diffusion systems – as opposed to *slowly linear* – has only been introduced relatively recently in the literature, in essence all explicit reaction-diffusion models considered in the earlier literature are of slowly linear type – see [28, 90]. Furthermore, it should be remarked there is no a priori reason to expect that localized solutions to singularly perturbed systems can only have $\mathcal{O}(1)$ amplitudes (w.r.t. ε). In [18], a scaling analysis allowing for amplitudes of a general asymptotic magnitude is performed in a general class of systems, the present scaling – and especially (4.10) with $\alpha(0) \neq 0$ – comes out as a natural 'normal form'.

By introducing the *fast variable* ξ through $x = \varepsilon\xi$, and redefining p by $\tilde{p} = \sqrt{\varepsilon}p$, (3.2) can be brought into its *fast* form,

$$\left\{ \begin{array}{rcl} u_\xi &=& \sqrt{\varepsilon}\tilde{p} \\ \tilde{p}_\xi &=& \sqrt{\varepsilon}\left[\varepsilon\mu u - \alpha\tilde{G}_2(u,v;\varepsilon)\right] \\ v_\xi &=& q \\ q_\xi &=& \nu v - H_2(u,v;\varepsilon) \end{array} \right. \tag{4.11}$$

In the limit $\varepsilon \downarrow 0$, this reduces to its *fast reduced limit*,

$$u = u_0,\ \tilde{p} = \tilde{p}_0,\ \ v_{\xi\xi} = \nu v - H_2(u_0, v; 0), \tag{4.12}$$

a 2-parameter family of integrable planar systems with saddle point $(0,0)$ (4.8). To construct a homoclinic solution in the full system (4.11), we need to assume leading order homoclinic behavior in (4.12), i.e. we need to assume that there is an open region $\mathcal{U}_0$ such that (4.12) has a homoclinic solution $v_{\mathrm{f-h}}(\xi; u_0)$ for all $u_0 \in \mathcal{U}_0$. Note that this is a natural and generic assumption – see section 4.2.1.

We now proceed in a more formal fashion. We introduce the region $\mathcal{I}_f = \{\xi \in (-1/\varepsilon^{1/4}, 1/\varepsilon^{1/4})\}$ that is equivalent to an x-domain of $\mathcal{O}(\varepsilon^{3/4})$ width and note that $v_{\mathrm{f-h}}(\xi; u_0)$ is exponentially small outside $\mathcal{I}_f$. (The precise asymptotic magnitude of $\mathcal{I}_f$ – i.e. the choice of the 'boundary' between the fast and slow subsystems – is not significant, other choices than the present are possible.) By assumptions (4.9), the slow component u satisfies a simple linear – *slow reduced* – equation in x outside $\mathcal{I}_f$,

$$u_{xx} - \mu u = 0 \tag{4.13}$$

(at leading order). Since we're looking for a homoclinic solution $\gamma_{\mathrm{h}}(\xi) = (u_{\mathrm{h}}(\xi), \tilde{p}_{\mathrm{h}}(\xi), v_{\mathrm{h}}(\xi), q_{\mathrm{h}}(\xi))$ of (4.11), we consider solutions $u(x)$ of (4.13) that $\to 0$ as $x \to \pm\infty$. We know from (4.11) that $u_\xi = \mathcal{O}(\sqrt{\varepsilon})$, which implies that $u(x)$ remains at leading order constant in the fast domain $\mathcal{I}_f$. Hence, we expect that the u-component of $\gamma_{\mathrm{h}}(\xi)$ is at leading order given by

$$u_{\mathrm{h}}(\xi) = \begin{cases} u_0 e^{+\varepsilon\sqrt{\mu}\xi}, & \xi < -1/\varepsilon^{1/4}, \\ u_0 e^{-\varepsilon\sqrt{\mu}\xi}, & \xi > +1/\varepsilon^{1/4}, \end{cases} \tag{4.14}$$

where u_0 a priori is a free parameter that corresponds directly to u_0 in (4.12) – the leading order value of u in $\mathcal{I}_f$. Note that the slow component of the homoclinic pulse in Fig. 4(b) indeed is of the form (4.14). To construct homoclinic pulse $\gamma_{\mathrm{h}}(\xi)$, we of course need to assume that u_0 is such that the fast reduced limit system (4.12) has a homoclinic solution $v_{\mathrm{f-h}}(\xi; u_0)$, i.e. that $u_0 \in \mathcal{U}_0$. In order to determine u_0 we note that approximation (4.14) implies that the derivative of $u_{\mathrm{h}}(\xi)$ must make an $\mathcal{O}(\varepsilon)$ *jump* as ξ varies over $\mathcal{I}_f$,

$$\Delta_{\mathrm{slow}} u_\xi = \lim_{\xi \downarrow -1/\varepsilon^{1/4}} u_{\mathrm{h},\xi}(\xi) - \lim_{\xi \uparrow 1/\varepsilon^{1/4}} u_{\mathrm{h},\xi}(\xi) = -2\varepsilon\sqrt{\mu} u_0 \tag{4.15}$$

(at leading order). This jump must be effectuated by the 'fast' evolution of u inside $\mathcal{I}_f$, i.e. by the accumulated change in u_ξ over $\mathcal{I}_f$,

$$\Delta_{\mathrm{fast}} u_\xi = \int_{\mathcal{I}_f} u_{\xi\xi} d\xi = -\varepsilon \int_{\mathcal{I}_f} \left(\alpha \tilde{G}_2(u, v; \varepsilon) - \varepsilon\mu u \right) d\xi = -\varepsilon\alpha \int_{-\infty}^{\infty} \tilde{G}_2(u_0, v_{\mathrm{f-h}}(\xi; u_0); 0) d\xi, \tag{4.16}$$

at leading order – where we have used the leading order approximations of u and v in $\mathcal{I}_f$ – and the (limited) asymptotic width of $\mathcal{I}_f$. Combining (4.15) and (4.16) yields an explicit (leading order) relation that determines u_0,

$$2\sqrt{\mu} u_0 = \alpha \int_{-\infty}^{\infty} \tilde{G}_2(u_0, v_{\mathrm{f-h}}(\xi; u_0); 0) d\xi. \tag{4.17}$$

Note that this expression can often be evaluated explicitly – such as the Gray-Scott and (generalized) Gierer-Meinhardt models – since the V-equation typically has the structure (in V) of the generalized Fischer-KPP equation (4.5) for which $v_{\mathrm{f-h}}(\xi; u_0)$ is known explicitly (4.6) – see for instance [18, 22].

To put the present formal construction into a rigorous framework – and to re-introduce the geometrical approach of (especially) section 4.1.2 – we need to 'translate' the above asymptotic analysis into the 'language' of *geometric singular perturbation theory*, or *Fenichel theory* [32, 43]. This goes beyond the scope of the present text, but we can give a brief sketch of this embedding.

First, we introduce the 2-dimensional invariant *slow manifold* $\mathcal{M}_\varepsilon$ of (4.11) that is simply given by $\{v = q = 0\}$ (and that is invariant by (4.9)); note that $\bar{P} = (0,0,0,0) \in \mathcal{M}_\varepsilon$. It follows by (4.8) that $\mathcal{M}_\varepsilon$ is *normally hyperbolic* [43], which implies – by Fenichel's Second Theorem – that both the 3-dimensional stable and unstable manifolds of $\mathcal{M}_\varepsilon$, $W^s(\mathcal{M}_\varepsilon)$ and $W^u(\mathcal{M}_\varepsilon)$ persist and that these are $\mathcal{O}(\sqrt{\varepsilon})$-close (in C^1) to their fast reduced limits given by the stable and unstable manifolds of the critical

point $(0,0)$ in (4.12) – i.e. the level sets of the associated Hamiltonian parameterized by $(u_0, \tilde{p}_0)$. Thus, $W^s(\mathcal{M}_\varepsilon)$ and $W^u(\mathcal{M}_\varepsilon)$ can be tracked with asymptotic accuracy and it can be shown by a Melnikov approach that $W^s(\mathcal{M}_\varepsilon)$ and $W^u(\mathcal{M}_\varepsilon)$ intersect transversally in a 2-dimensional submanifold – recall that 3-dimensional manifolds in $\mathbb{R}^4$ are expected to have 2-dimensional intersections. This intersection represents a 1-parameter family of solutions to (4.11) that are homoclinic to $\mathcal{M}_\varepsilon$. This implies that the homoclinic solution $\gamma_{\rm h}(\xi) \subset W^u(\bar{P}) \cap W^s(\bar{P}) \subset W^u(\mathcal{M}_\varepsilon) \cap W^s(\mathcal{M}_\varepsilon)$ we're looking for is an element of this family. Next, it follows by Fenichel's Third Theorem that there is a curve $\mathcal{T}_{\rm off} \subset \mathcal{M}_\varepsilon$ from which these orbits 'take off' (from $\mathcal{M}_\varepsilon$) and a (symmetric) curve $\mathcal{T}_{\rm down} \subset \mathcal{M}_\varepsilon$ at which the orbits 'touch down' (on $\mathcal{M}_\varepsilon$) again – after a 'circuit through the fast field'. Moreover, $\mathcal{T}_{\rm off}$ and $\mathcal{T}_{\rm down}$ can be determined/approximated explicitly. The (symmetric) homoclinic orbit $\gamma_{\rm h}(\xi)$ must correspond to an intersection of the restriction of $W^u(\bar{P})$ to $\mathcal{M}_\varepsilon$ – i.e. $W^u(\bar{P}) \cap \mathcal{M}_\varepsilon$ – with $\mathcal{T}_{\rm off}$ (or equivalently by symmetry (3.3) to points in $\big(W^s(\bar{P}) \cap \mathcal{M}_\varepsilon\big) \cap \mathcal{T}_{\rm down}$). In analytical terms, this intersection condition is given by the above derived jump relation (4.17).

Based on this geometric framework, we may thus formulate a theorem on the existence of homoclinic pulses – that's in fact a special case of Theorem 2.1 in [28] on the existence of homoclinic pulses in *slowly nonlinear* systems. We thus refer to [28] for the geometric 'details' of the proof (and for a much more precise formulation).

Theorem 4.7 *Assume that u_0^* is a non-degenerate solution of (4.17) and that assumptions (4.8), (4.9) hold, and let $\varepsilon > 0$ be sufficiently small, then system (4.11) has a symmetric solution $\gamma_{\rm h}(\xi)$ that is homoclinic to $\bar{P} = (0,0,0,0)$. Moreover, the U-component of the associated homoclinic pulse pattern $(U_{\rm h}(x), V_{\rm h}(x))$ in (1.2) is at leading order given by (4.14), the V-component by the homoclinic solution $v_{\rm f-h}(\xi; u_0)$ of (4.12) – where $u_0 = u_0^*$ in both cases.*

Remark 4.8 A result similar to that of Theorem 4.7 can be obtained for a family of spatially periodic solutions $\gamma_{\rm p}(\xi;\sigma)$/spatially periodic patterns $(U_{\rm p}(x;\sigma), V_{\rm p}(x;\sigma))$ that limits on $\gamma_{\rm h}(\xi)/(U_{\rm h}(x), V_{\rm h}(x))$ as period $T(\sigma) \to \infty$ – see Fig. 4(c) and Lemma 4.5. Here, the situation is a bit more subtle since $\gamma_{\rm p}(\xi;\sigma)$ is not a subset of $W^s(\mathcal{M}_\varepsilon) \cap W^u(\mathcal{M}_\varepsilon)$ (but exponentially close to it). We refrain from going into the details and refer to [15] for a (much more) general existence result and to [21] for a deeper exploration into the extremely rich structure of periodic (and aperiodic) symmetric solutions to singularly perturbed 2-component reaction-diffusion systems.

4.3 The stability of stationary pulse solutions

Of course, the next question is whether the homoclinic pulse patterns constructed in the previous section may be stable (and thus 'observable'). We again first consider the scalar problem.

4.3.1 The scalar problem

The (linearized) stability of a stationary pulse pattern $U(x,t) = u_{\rm h}(x)$ – a homoclinic solution $(u_{\rm h}(x), p_{\rm h}(x))$ of spatial system (4.1) – is determined by the spectral problem obtained by linearizing about the pulse, i.e. by substituting $U(x,t) = u_{\rm h}(x) + e^{\lambda t} u(x)$ into (1.1) (with $N = n = 1$) and neglecting all nonlinear effects,

$$\mathcal{L}u = \lambda u \quad \text{with} \quad \mathcal{L} = \mathcal{L}(x;\mu) = \frac{d^2}{dx^2} + F'(u_{\rm h}(x);\mu). \tag{4.18}$$

This is a degenerate Sturm-Liouville problem (defined on $\mathbb{R}$), its spectrum consist of two parts,

$$\text{spec}(\mathcal{L}) = \sigma_{\rm ess} \cup \sigma_{\rm discr} = (-\infty, f_u) \cup \{\lambda_0, ..., \lambda_J\} \text{ with } f_u = \frac{dF}{dU}(\bar{U}) < \lambda_J < ... < \lambda_0, \tag{4.19}$$

for some bounded $J \geq 1$ [45] – where we note that $\sigma_{\rm ess}$ cannot cause an instability since $(\bar{U}, 0) = \lim_{x\to\pm\infty}(u_{\rm h}(x), p_{\rm h}(x))$ is a saddle, hence $f_u < 0$ (section 4.1.1). Note also that $J = 2$ for the classical case $\mu = 2$ in the F-KPP equation (4.5) – with $\lambda_0 = 5/4, \lambda_1 = 0, \lambda_2 = -3/4$ – and that $J = J(\mu) \uparrow \infty$ as $\mu \downarrow 1$ in (4.5)-(gFKPP) [18]. Since $0 = \frac{d}{dx}(u_{{\rm h},xx} + F(u_{\rm h}))$, it follows that $\mathcal{L}(u_{{\rm h},x}) = 0$: $\lambda = 0$ is an eigenvalue of $\mathcal{L}$. Moreover, the eigenfunction $u_j(x)$ associated to the jth eigenvalue λ_j of (4.18) has j zeroes [45], since $u_{{\rm h},x}$ clearly has exactly one zero, this implies that $\lambda_1 = 0$, so that $\lambda_0 > 0$.

Theorem 4.9 *Any stationary homoclinic pulse solution* $u_{\rm h}(x)$ *of (1.1)* with $N = 1$ *must be* unstable.

A similar result certainly does not hold for heteroclinic fronts. In fact, both heteroclinic connections in the Nagumo model (4.5) for $\mu = 1/2$ are monotonic: $u_{{\rm h},x}$ does not have zeroes and $\lambda_0 = 0$. Since for h small,

$$u_{\rm h}(x+h) = u_{\rm h}(x) + u_{{\rm h},x}(x)h + \mathcal{O}(h^2),$$

it follows that the eigenvalue $\lambda = 0$ is associated to the translation invariance in (1.1) – *this is also the case for general N-component localized structures.* It is thus 'harmless' [45] and it follows that both (stationary) fronts in (4.5)-(N) are spectrally stable, and as a consequence stable [45]. In fact, by going into a moving coordinate frame $\xi = x - ct$ one can show that the Nagumo model (4.5-(N) has a travelling front for any $\mu \in (0,1)$ – with speed explicitly given by $c = \frac{1}{2}\sqrt{2}(1-2\mu)$ [57]. Subsequently, one can apply Sturm-Liouville theory to show that $\lambda_j < \lambda_0 = 0$ for all $j = 1, ..., J$: the travelling fronts solutions of the Nagumo model are all stable. *A similar result can be established in general for travelling fronts in scalar RDEs* [45].

4.3.2 The spectral stability problem

Before we focus on the singularly perturbed case of section 4.2.2 and Theorem 4.7, we first consider the more general setting. Thus, we assume we have a stationary symmetric homoclinic pulse solution $(U_{\rm h}(x), V_{\rm h}(x))$ of (1.2) that limits on the stable background state $(\bar{U}, \bar{V})$ as $x \to \pm\infty$. To investigate its spectral stability we set,

$$(U(x,t), V(x,t)) = (U_{\rm h}(x), V_{\rm h}(x)) + (u(x), v(x))\, e^{\lambda t} \quad \text{with} \quad \lambda \in \mathbb{C} \tag{4.20}$$

(cf. (2.1)), with $u, v : \mathbb{R} \to \mathbb{C}$ not to be confused with the real valued $(u(x), v(x))$ introduced in (3.1). Substitution of (4.20) into (1.2) yields a linear spectral stability problem which can be written in several equivalent ways. First, we may choose to stress the idea that a 2-component problem can be seen as 2 coupled scalar problems (this will be useful in the singularly perturbed setting of section 4.3.3),

$$\left\{ \begin{array}{rcl} u_{xx} + \left(\frac{\partial G}{\partial U}(U_{\rm h}(x), V_{\rm h}(x); \mu) - \lambda\right) u & = & -\frac{\partial G}{\partial V}(U_{\rm h}(x), V_{\rm h}(x); \mu) v, \\ d v_{xx} + \left(\frac{\partial H}{\partial V}(U_{\rm h}(x), V_{\rm h}(x); \mu) - \lambda\right) v & = & -\frac{\partial H}{\partial U}(U_{\rm h}(x), V_{\rm h}(x); \mu) u. \end{array} \right. \tag{4.21}$$

However, this point of view obscures the fact that a multi-component spectral stability problem differs significantly from a scalar (Sturm-Liouville) problem. Therefore, we introduce the matrix differential operator $\mathbb{L} = \mathbb{L}(x; \mu)$ and formulate the spectral stability problem as,

$$\mathbb{L}(x;\mu) \begin{pmatrix} u \\ v \end{pmatrix} = \lambda \begin{pmatrix} u \\ v \end{pmatrix}, \tag{4.22}$$

with

$$\mathbb{L}(x;\mu) = \begin{pmatrix} \frac{d^2}{dx^2} + \frac{\partial G}{\partial U}(U_{\rm h}(x), V_{\rm h}(x); \mu) & \frac{\partial G}{\partial V}(U_{\rm h}(x), V_{\rm h}(x); \mu) \\ \frac{\partial H}{\partial U}(U_{\rm h}(x), V_{\rm h}(x); \mu) & d\frac{d^2}{dx^2} + \frac{\partial H}{\partial V}(U_{\rm h}(x), V_{\rm h}(x); \mu) \end{pmatrix}, \tag{4.23}$$

and immediately observe that $\mathbb{L}(x;\mu)$ is not self-adjoint (in general): unlike the scalar case, the spectrum of $\mathbb{L}$ is not necessarily real. Nevertheless, also in this setting a spectral decomposition like (4.19) can be made,

$$\text{spec}(\mathbb{L}) = \sigma_{\rm ess} \cup \sigma_{\rm discr} = \sigma_{\rm ess}((\bar{U}, \bar{V})) \cup \{\lambda_0, ..., \lambda_J\}, \tag{4.24}$$

in which $\sigma_{\rm ess}((\bar{U}, \bar{V}))$ is the spectrum associated to the stability of the background state $(\bar{U}, \bar{V})$ that has been determined in detail in section 2.1 – see again [45]. Since we focus on pulse solutions $(U_{\rm h}(x), V_{\rm h}(x))$ that are homoclinic to stable background states, we may conclude that their spectral stability is determined by the eigenvalues $\lambda_0, ..., \lambda_J \in \mathbb{C}$ – where we once again note that these λ_j's are not necessarily real. The method of *the Evans function* – see [1, 45, 70] and the upcoming section 4.3.3 – has been developed to determine these eigenvalues λ_j. It starts with a third way to formulate the spectral stability problem: as a 4-dimensional dynamical system,

$$\Phi_x = \mathcal{B}_{\rm h}(x; \lambda, \mu)\Phi, \tag{4.25}$$

in which $\Phi = (u, p, v, q) : \mathbb{R} \to \mathbb{C}^4$ and,

$$\mathcal{B}_{\rm h}(x;\lambda,\mu) = \begin{pmatrix} 0 & 1 & 0 & 0 \\ \lambda - \frac{\partial G}{\partial U}(U_{\rm h}(x), V_{\rm h}(x);\mu) & 0 & -\frac{\partial G}{\partial V}(U_{\rm h}(x), V_{\rm h}(x);\mu) & 0 \\ 0 & 0 & 0 & \frac{1}{\sqrt{d}} \\ -\frac{1}{\sqrt{d}}\frac{\partial H}{\partial U}(U_{\rm h}(x), V_{\rm h}(x);\mu) & 0 & \frac{1}{\sqrt{d}}\left(\lambda - \frac{\partial H}{\partial V}(U_{\rm h}(x), V_{\rm h}(x);\mu)\right) & 0 \end{pmatrix}. \tag{4.26}$$

The limit matrix $\mathcal{B}_\infty(\lambda;\mu) = \lim_{x\to\pm\infty} \mathcal{B}_{\rm h}(x;0,\mu)$, with

$$\mathcal{B}_\infty(\lambda;\mu) = \begin{pmatrix} 0 & 1 & 0 & 0 \\ \lambda - g_u & 0 & -g_v & 0 \\ 0 & 0 & 0 & \frac{1}{\sqrt{d}} \\ -\frac{1}{\sqrt{d}}h_u & 0 & \frac{1}{\sqrt{d}}(\lambda - h_v) & 0 \end{pmatrix} \tag{4.27}$$

(2.3) plays a central role in the Evans function approach. Its eigenvalues $\Lambda_j(\lambda;\mu)$ are determined by,

$$\Lambda^4 + \frac{1}{d}\left[(dg_u + h_v) - (d+1)\lambda\right]\Lambda^2 + \frac{1}{d}\left[(g_u h_v - g_v h_u) + (\lambda^2 - (g_u + h_v)\lambda)\right] = 0. \tag{4.28}$$

Since clearly $\mathcal{B}_\infty(0,\mu) = \mathcal{B}(\mu)$ (4.2), this characteristic polynomial reduces to (4.3) at $\lambda = 0$. Moreover, (4.28) can equivalently be written in a form similar to the 2×2 characteristic polynomial (2.4) associated to the spectral stability of the limit state $(\bar{U}, \bar{V})$,

$$\lambda^2 - \left[(g_u + h_v) + (1+d)\Lambda^2\right]\lambda + \left[(g_u + \Lambda^2)(h_v + d\Lambda^2) - g_v h_u\right] = 0. \tag{4.29}$$

For purely imaginary values of Λ – i.e. for $\Lambda = ik \in i\mathbb{R}$ – this equation is *identical* to (2.4). By comparing (4.20) to (2.1) and interpreting the spatial eigenvalues Λ of $\mathcal{B}_\infty$ – the $x \to \pm\infty$ evaluation of $\mathcal{B}_{\rm h}(x)$ at $(\bar{U}, \bar{V})$ – in terms of (2.1), it follows that this indeed must be the case (by construction). In fact, this observation provides a natural embedding of the relation between purely imaginary eigenvalues Λ of (4.3) and solutions $\lambda(k) = 0$ of (2.4) as discussed in section 4.1.1. Moreover, it implies that for all $\lambda \notin \sigma_{\rm ess}((\bar{U}, \bar{V}))$ – the continuous component of spec($\mathbb{L}$) (4.24) – the spatial eigenvalues $\Lambda(\lambda;\mu)$ must have $\mathrm{Re}(\Lambda(\lambda;\mu)) \neq 0$. Since (4.28) is a quadratic equation in $\ell = \Lambda^2$ – like (4.3) – it follows that the eigenvalues of $\mathcal{B}_\infty(\lambda;\mu)$ can be ordered as,

$$\mathrm{Re}\left(\Lambda_1(\lambda;\mu)\right) \geq \mathrm{Re}\left(\Lambda_2(\lambda;\mu)\right) > 0 > \mathrm{Re}\left(\Lambda_3(\lambda;\mu)\right) \geq \mathrm{Re}\left(\Lambda_4(\lambda;\mu)\right), \tag{4.30}$$

for all $\lambda \notin \sigma_{\rm ess}((\bar{U}, \bar{V}))$. This is the foundation on which the Evans function approach is built.

4.3.3 Stability analysis in singularly perturbed systems

The Evans function set-up can be further elaborated for general systems [1, 45, 70], however, the situation is similar to the existence problem: the Evans function approach has a strong geometrical character, to evaluate it one needs to control certain manifolds. As in the existence problem, there in general is no 'tool' by which these manifolds can be traced, which implies that there is in general no way to *explicitly* determine the discrete spectrum of $\mathbb{L}$. Hence, there is no general way to establish the stability of a homoclinic pulse pattern $(U_{\rm h}(x), V_{\rm h}(x))$ of (1.2).

Such control is – again – possible in the setting of singularly perturbed systems. Thus, as in section 4.2.2 we assume that $0 < d = \varepsilon^2 \ll 1$ in (1.2), shift $(\bar{U}, \bar{V})$ to $(0,0)$ and impose assumptions (4.7)–(4.10). (And we again note that similar results as presented below can be obtained in a much more general setting [28].) Theorem 4.7 thus provides a (stationary, symmetric, singular) pulse pattern $(U_{\rm h}(x), V_{\rm h}(x))$ – for ε sufficiently small, if there is a solution u_0^* to (4.17) – and we first study its spectral stability problem by a formal approach – which is remarkably similar to that of section 4.2.2.

Since the fast spatial interval $\mathcal{I}_f$ is asymptotically small (in x), it follows that the u component of an eigenfunction remains (at leading order) constant over $\mathcal{I}_f$. Moreover, since the stability problem is linear, we may set this constant equal to 1 (we thus exclude the possibility that $u(0) = 0$, which cannot happen,

see below (4.34)). By the explicit approximations given in Theorem 4.7 and assumptions (4.7) and (4.8), we deduce that the v-equation in (4.21) is, at leading order and in the fast spatial coordinate ξ, given by,

$$v_{\xi\xi} + \left(\frac{\partial H_2}{\partial V}(u_0^*, v_{\mathrm{f-h}}(\xi; u_0^*)) - (\nu + \lambda)\right) v = -\frac{\partial H_2}{\partial U}(u_0^*, v_{\mathrm{f-h}}(\xi; u_0^*)), \tag{4.31}$$

the *fast reduced limit* of the stability problem. Now, we may interpret fast reduced problem (4.12) as the existence problem associated to the scalar equation,

$$V_t = V_{\xi\xi} - \nu V + H_2(u_0, V; 0), \tag{4.32}$$

that has a homoclinic orbit $v_{\mathrm{f-h}}(\xi; u_0)$ (section 4.2.2). The spectral stability of $v_{\mathrm{f-h}}(\xi; u_0)$ as solution of (4.32) is determined by the linear operator $\mathcal{L}_{\mathrm{f-h}}(\xi; u_0)$ – which is defined as $\mathcal{L}(x)$ in (4.18). This is a Sturm-Liouville operator (section 4.3.1) and we may thus assume that we know its spectrum – see (4.19) and [45]; we denote its eigenvalues by $\lambda_{\mathrm{f-h},j}(u_0)$, $j = 0, ..., J$. The fast reduced stability problem (4.31) can now be written as an inhomogeneous problem in $\mathcal{L}_{\mathrm{f-h}}(\xi; u_0)$. For any $\lambda \neq \lambda_{\mathrm{f-h},j}(u_0)$, $j = 0, ..., J$, this problem has a unique, exponentially decaying solution $v_{\mathrm{in}}(\xi; \lambda, u_0^*)$,

$$v_{\mathrm{in}}(\xi; \lambda, u_0^*) = -\left(\mathcal{L}_{\mathrm{f-h}}(\xi; u_0^*) - \lambda\right)^{-1} \left(\frac{\partial H_2}{\partial U}(u_0^*, v_{\mathrm{f-h}}(\xi; u_0^*))\right), \tag{4.33}$$

[28, 45]. By the exponential decay (in ξ) of both $v_{\mathrm{f-h}}(\xi; u_0^*)$ and $v_{\mathrm{in}}(\xi; \lambda, u_0^*)$ and using assumptions (4.7)-(4.9) in (4.21), we find that, outside $\mathcal{I}_f$, the stability problem in u is (at leading order) given by the *slow reduced limit*,

$$u_{xx} - (\mu + \lambda)u = 0, \tag{4.34}$$

which can be solved as its almost identical counterpart (4.13) in (4.14). There is, however, one essential difference with (4.14): unlike the existence problem, system (4.21) is linear, which implies that the exact value of $u(x)$ over $\mathcal{I}_f$ is irrelevant; it cannot be 0 – this would imply $u(x) \equiv 0$ – and can thus be scaled to 1. We can now proceed in a way that is *identical* to section 4.2.2. We note that the ξ-derivative of $u(\xi)$ makes an $\mathcal{O}(\varepsilon)$ *jump* as ξ varies over $\mathcal{I}_f$ that is at leading order given by,

$$\Delta_{\mathrm{slow}} u_\xi = -2\varepsilon\sqrt{\mu + \lambda} \tag{4.35}$$

(cf. (4.15)). Also here, this jump must be caused by the 'fast' evolution of u inside $\mathcal{I}_f$, i.e. by the accumulated change in u_ξ over $\mathcal{I}_f$. Following (4.16), we find that this is at leading order given by,

$$\Delta_{\mathrm{fast}} u_\xi = -\varepsilon\alpha \int_{-\infty}^{\infty} \left(\frac{\partial \tilde{G}_2}{\partial U}(u_0^*, v_{\mathrm{f-h}}(\xi; u_0^*)) + \frac{\partial \tilde{G}_2}{\partial V}(u_0^*, v_{\mathrm{f-h}}(\xi; u_0^*)) v_{\mathrm{in}}(\xi; \lambda, u_0^*)\right) d\xi, \tag{4.36}$$

where we have introduced α and $\tilde{G}_2(U, V)$ in (4.21) by (4.7) and (4.10) and used the fact that $v(\xi)$ is at leading order given by $v_{\mathrm{in}}(\xi; \lambda, u_0^*)$ (4.33). By 'matching' (4.35) to (4.36) we find the counterpart of (4.17),

$$2\sqrt{\mu + \lambda} = \alpha \int_{-\infty}^{\infty} \left(\frac{\partial \tilde{G}_2}{\partial U}(u_0^*, v_{\mathrm{f-h}}(\xi; u_0^*)) + \frac{\partial \tilde{G}_2}{\partial V}(u_0^*, v_{\mathrm{f-h}}(\xi; u_0^*)) v_{\mathrm{in}}(\xi; \lambda, u_0^*)\right) d\xi. \tag{4.37}$$

This is an explicit relation in terms of λ; the Evans function approach establishes that the solutions of (4.37) determine the spectral stability of the pulse pattern $(U_{\mathrm{h}}(x), V_{\mathrm{h}}(x))$. Once again as in the case of the existence problem, we refrain from going into the 'details' of the full construction of the Evans function – by which the above formal analysis and the decisive relevance of (4.37) can be established: it goes beyond the scope of the present text. However, we can – again – provide a sketch.

To do so, we start with the eigenvalues $\Lambda_j(\lambda; \mu)$ of $\mathcal{B}_\infty(\lambda; \mu)$ (4.27) that can be ordered like (4.30) for all $\lambda \in \mathbb{C} \backslash \sigma_{\mathrm{ess}}((\bar{U}, \bar{V}))$ (section 4.3.2). It can be shown – it is in fact quite natural – that there are 4 solutions $\Phi_j(x; \lambda, \mu)$, $j = 1, ..., 4$ of the full stability problem (4.25) that behave like the eigenvector solutions of the constant coefficient problem associated to $\mathcal{B}_\infty(\lambda; \mu)$ as $x \to \pm\infty$. More precise, define $E_j(\lambda; \mu)$ as the

eigenvectors of $\mathcal{B}_\infty(\lambda;\mu)$ associated to eigenvalues $\Lambda_j(\lambda;\mu)$, then it follows that there are eigensolutions $\Phi_j(x;\mu)$ of (4.25) such that,

$$\begin{array}{ll} \lim_{x\to-\infty}\Phi_1(x;\lambda,\mu)e^{-\Lambda_1(\lambda;\mu)x}=E_1(\lambda;\mu), & \lim_{x\to-\infty}\Phi_2(x;\lambda,\mu)e^{-\Lambda_2(\lambda;\mu)x}=E_2(\lambda;\mu),\\ \lim_{x\to+\infty}\Phi_3(x;\lambda,\mu)e^{-\Lambda_3(\lambda;\mu)x}=E_3(\lambda;\mu), & \lim_{x\to+\infty}\Phi_4(x;\lambda,\mu)e^{-\Lambda_4(\lambda;\mu)x}=E_4(\lambda;\mu). \end{array}$$

[18, 28]. Thus, for $\lambda\notin\sigma_{\rm ess}((\bar U,\bar V))$, $\Psi_-=\text{span}\{\Phi_1,\Phi_2\}$ and $\Psi_+=\text{span}\{\Phi_3,\Phi_4\}$ are 2-dimensional linear manifolds of solutions to (4.25) that decay to 0 as $x\to-\infty$ or as $x\to\infty$. Together, $(\Phi_1,\Phi_2,\Phi_3,\Phi_4)$ may form a fundamental matrix solution of (4.25). The Evans function $\mathcal{D}(\lambda;\mu)$ is defined as the determinant,

$$\mathcal{D}(\lambda;\mu)=\ \det(\Phi_1(x;\lambda,\mu),\Phi_2(x;\lambda,\mu),\Phi_3(x;\lambda,\mu),\Phi_4(x;\lambda,\mu)).$$

$\mathcal{D}(\lambda;\mu)$ does not depend on x (by Abel's Theorem) and is *analytic* as function of $\lambda\in\mathbb{C}\backslash\sigma_{\rm ess}((\bar U,\bar V))$ [1, 45]. A zero of $\mathcal{D}(\lambda)$ corresponds to an intersection of Ψ_- and Ψ_+, which determines a solution of (4.25) that decays for both $x\to\pm\infty$: an eigenfunction of (4.21)/(4.22)/(4.25). In other words, zeroes of $\mathcal{D}(\lambda;\mu)$ correspond to eigenvalues of (4.21)/(4.22)/(4.25) (counting multiplicities) [1, 45].

In the context of the singularly perturbed systems considered here, $\mathcal{D}(\lambda;\varepsilon)$ – where we again suppress the μ dependence – can be decomposed into *the product of a fast and a slow Evans function*, $\mathcal{D}(\lambda;\varepsilon)=\mathcal{D}_{\rm f}(\lambda;\varepsilon)\mathcal{D}_{\rm s}(\lambda;\varepsilon)$ [1, 18, 28]. Like $\mathcal{D}(\lambda;\varepsilon)$, $\mathcal{D}_{\rm f}(\lambda;\varepsilon)$ is analytic in $\mathbb{C}\backslash\sigma_{\rm ess}((\bar U,\bar V))$, its zeroes are given by the eigenvalues $\lambda_{{\rm f-h},j}$ of the operator $\mathcal{L}_{\rm f-h}(\xi)$ associated to the scalar problem (4.32) [1]. However, the slow Evans function $\mathcal{D}_{\rm s}(\lambda;\varepsilon)$ is *meromorphic*, it may have poles at the zeroes of $\mathcal{D}_{\rm f}(\lambda;\varepsilon)$ – the eigenvalues $\lambda_{{\rm f-h},j}$ [18, 28]. This is especially the case for the critical eigenvalue $\lambda_{{\rm f-h},0}>0$ (section 4.3.1): $\lambda_{{\rm f-h},0}$ is a pole of $\mathcal{D}_{\rm s}(\lambda;\varepsilon)$ and thus not a zero of the full Evans function $\mathcal{D}(\lambda;\varepsilon)$, *it is not an (unstable) eigenvalue* [18, 28]. Hence, unlike in the scalar case – Theorem 4.9 – homoclinic pulses may be stable in the 2-component setting of (1.2). The stability of the pulse is $(U_{\rm h}(x),V_{\rm h}(x))$ is thus decided by the zeroes of $\mathcal{D}_{\rm s}(\lambda;\varepsilon)$, that are determined by (4.37) [28] (since the above formal construction provides a (leading order) solution of (4.21)/(4.22)/(4.25) that decays to 0 as $x\to\pm\infty$, i.e. an element of $\Psi_-\cap\Psi_+$).

Theorem 4.10 *Let all conditions and assumptions of Theorem 4.7 hold and let $(U_{\rm h}(x),V_{\rm h}(x))$ be a homoclinic pulse pattern constructed in Theorem 4.7. Except for the translational eigenvalue $\lambda=\lambda_{{\rm f-h},1}=0$ and the stable eigenvalues $\lambda_{{\rm f-h},2j}<0$ ($j>0$), all eigenvalues associated to the spectral stability of $(U_{\rm h}(x),V_{\rm h}(x))$ are determined by $\mathcal{D}_{\rm s}(\lambda;\varepsilon)=0$, and thus by (4.37). More specifically, if all solutions $\lambda\in\mathbb{C}\backslash\sigma_{\rm ess}((\bar U,\bar V))$ of (4.37) have* $\text{Re}(\lambda)<0$*, then $(U_{\rm h}(x),V_{\rm h}(x))$ is stable as solution of (1.2).*

As for Theorem 4.7, the details can be found in [28], in which a more general – slowly nonlinear – and more carefully formulated result is established (see Theorem 4.4 in [28]; in fact (4.37) appears as 'linear limit' in Corollary 4.5 of [28]). Since operator $\mathbb{L}(x;\varepsilon)$ (4.23) is sectorial, nonlinear stability follows 'automatically' from spectral stability [41, 45].

Thus – similar to the existence problem – in the singularly perturbed case we have deduced an *explicit* expression by which the stability of a pulse $(U_{\rm h}(x),V_{\rm h}(x))$ can be established. However, especially due to the appearance of $v_{\rm in}(\xi;\lambda)$, (4.37) of Theorem 4.10 seems like an expression that is (too) hard to evaluate/understand – unlike (4.17) in Theorem 4.7. This is not the case, however, in large families of systems with Gray-Scott/Gierer-Meinhardt type nonlinearities $H_2(U,V)$: for these systems, nonhomogeneous equation (4.31) can be solved explicitly – i.e. $v_{\rm in}(\xi;\lambda)$ can be explicitly determined – in terms of hypergeometric and/or associated Legendre functions [17, 18, 28] (see [17, 18, 28, 91]). Moreover, one can also deduce several instability results – often based on the geometrical nature of the intersections $W^u(\mathcal{M}_\varepsilon)\cap W^s(\mathcal{M}_\varepsilon)$ through which the pulse pattern is constructed (section 4.2.2) – see [28]. Here, we mention one of the most simple of these – that validates the introduction of $\alpha(\varepsilon)$ in (4.10).

Corollary 4.11 *Let $\alpha(\varepsilon)$ be as defined in (4.10) and let ε be sufficiently small. Then, there is an $\alpha_0>0$ such that all pulse patterns $(U_{\rm h}(x),V_{\rm h}(x))$ as constructed in Theorem 4.7 are* unstable *for $|\alpha(\varepsilon)|<\alpha_0$.*

Proof (rough sketch). Since the operator $(\mathcal{L}_{\rm f-h}(\xi)-\lambda)$ is not invertible at the critical eigenvalue $\lambda_{{\rm f-h},0}>0$, the right hand side of (4.37) must have a simple pole/non-degenerate vertical asymptote at $\lambda=\lambda_{{\rm f-h},0}$. Thus, for α sufficiently small, the 2 curves determined by the left and right hand sides of (4.37) must intersect near $\lambda_{{\rm f-h},0}>0$ – which implies instability by Theorem 4.10. □

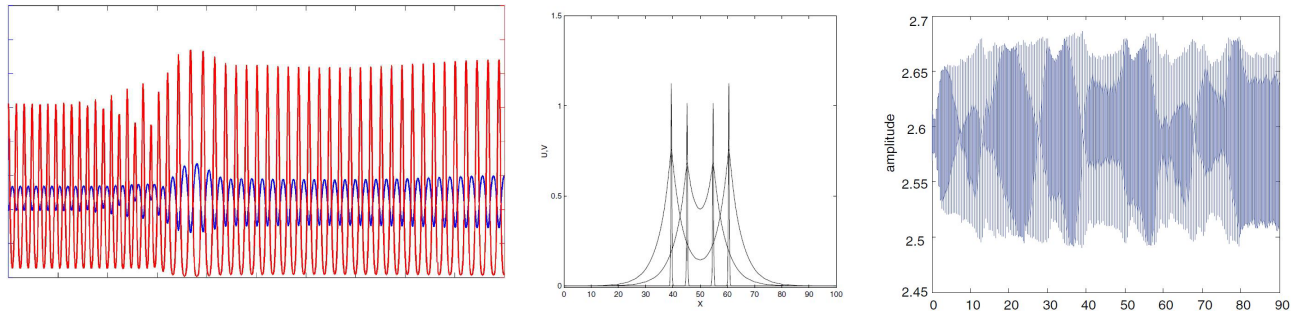

Figure 5: (a) Strong interactions in the Gray-Scott model: a travelling period-doubling invasion front. (b) From [20]: the semi-strong evolution of a 2-pulse pattern in the Gierer-Meinhardt equation in 2 snapshots. (c) From [91]: Chaotic oscillations of the maximum of a standing pulse in a simulation of a slowly nonlinear model.

Remark 4.12 Like in the existence case (i.e. like in Remark 4.8), a result similar to that of Theorem 4.10 can be obtained for a family of spatially periodic patterns $(U_{\rm p}(x;\sigma), V_{\rm p}(x;\sigma))$ that limits on $(U_{\rm h}(x), V_{\rm h}(x))$ as period $T(\sigma) \to \infty$ – see Fig. 4(c) and Lemma 4.5. This can be done using the Floquet theory based concept of γ-eigenvalues [35] – see [15] (also for a much more general setting than considered here).

Remark 4.13 Both the geometric singular perturbation approach to the (singularly perturbed) existence problem of section 4.2.2 and the Evans function approach to the (singularly perturbed) spectral stability problem of section 4.3.3 have been originally developed by Chris Jones in the context of travelling pulses in the FitzHugh-Nagumo model – a singularly perturbed 2-component reaction-diffusion model of type (1.2) in which d is typically set 0 – see [42, 43]. These days, the FitzHugh-Nagumo model continues to serve as a paradigmatic equation in which new approaches to new types of patterns are developed – see for instance the travelling waves with oscillating tails of [8, 9] and section 5.1.2.

5 Complex pattern dynamics

In this section we give a *brief* overview of the types of patterns observed and studied beyond the most simple ones considered so far. As in this entire text, we focus on the mathematical 'tools' available to understand the complexity of these patterns.

5.1 In $\mathbb{R}^1$

5.1.1 Pulse interactions

Especially in the context of singularly perturbed RDEs – $0 < d \ll 1$ or $d \gg 1$ in (1.2) – the evolution of the patterns generated by (1.2) can often be seen (and understood) in terms of interacting localized structures – see for instance Fig. 1(c). In general, one distinguishes two types of pulse or front interactions: *weak interactions* and *strong interactions*. As usual in this text we focus for simplicity on pulses: let $(U_{\rm h}(x), V_{\rm h}(x))$ be an asymptotically stable stationary homoclinic pulse solution of (1.2) and consider the *approximate* evolving J-pulse pattern consisting of J identical but translated copies of $(U_{\rm h}(x), V_{\rm h}(x))$,

$$\begin{pmatrix} U(x,t) \\ V(x,t) \end{pmatrix} = \Sigma_{j=1}^{J} \begin{pmatrix} U_{\rm h}(x - x_j(t)) \\ V_{\rm h}(x - x_j(t)) \end{pmatrix}. \tag{5.38}$$

Of course, (5.38) cannot describe an exact solution of (1.2), but under the assumptions that the 'tails' of $(U_{\rm h}(x), V_{\rm h}(x))$ decay exponentially fast and that the distances $|x_i(t) - x_j(t)|$ between the pulses are sufficiently large (for all $i, j = 1, ..., J$), (5.38) provides an accurate leading order approximation, *if the pulse-positions $x_j(t)$ satisfy a certain (simple) J-dimensional ODE* that can be determined explicitly by projecting the flow generated by (1.2) on the J-dimensional subspace spanned by the derivatives $(U_{{\rm h},x}(x - x_j), V_{{\rm h},x}(x - x_j))$ of the J constituting pulses. In fact, it can be shown rigorously that, as long as $|x_i(t) - x_j(t)|$ remains sufficiently large – i.e. as long as the pulses are in *weak interaction* – the infinite-dimensional flow associated to (1.2) can be reduced to an asymptotically attracting J-dimensional invariant manifold on

which the flow is governed by the J equations for $\dot{x}_j$ – see [31, 64, 70, 96]. In this weak interaction setting, the pulses behave as 'particles' – only their position $x_j(t)$ varies in time, their shape and stability characteristics do not change (up to exponentially small effects).

Contrary to the weak case, there is virtually no general mathematical theory on *strong* pulse (or front) interactions in reaction-diffusion systems (see [7, 34] for subtle analytical treatments of strong interactions in singularly perturbed *scalar* equations). Strong interaction is the conglomerating term for interactions in which localized structures 'change significantly'. In the setting of pulses, examples include merging pairs of pulses that continue as 1 pulse, pulses that 'disappear' or get 'annihilated', pulses that 'self-replicate' and evolve into a pair of repulsive pulses, etc. See for instance the simulations of self-replicating pulses in the 1-dimensional Gray-Scott model in [22, 67] and especially in [62], in which an example is given of spatio-temporal chaos driven by subsequently annihilating and self-replicating pulses; see also Fig. 5(a) in which a period doubling bifurcation – see section 3.2 – takes place through an invasion wave annihilating every second pulse.

In the setting of singularly perturbed reaction-diffusion systems, the intermediate concept of *semi-strong* (pulse) interactions has been introduced in [19]: pulses that interact weakly through their 'fast' component(s) and strongly through their slow component(s) – see Figs. 1(b) and 5(b). Although the theory is less well-developed than in the weak case, there are similar rigorous results on the reduction of the full PDE-flow to an approximate finite-dimensional manifold – with boundaries [3, 20]; moreover, the ODEs governing the finite-dimensional dynamics can also be determined explicitly [10, 19, 93]. Very unlike the weak interaction case, pulses change shape during the evolution – see Fig. 5(b) – and their stability characteristics – i.e. their 'quasi-steady spectrum' – changes through the interactions. In fact, the boundaries of the manifold on which the pulse interaction problem takes place are formed by situations in which this quasi-steady spectrum approaches the imaginary axis [3]. Of course, the most interesting pulse dynamics takes place near these boundaries. This is the subject of ongoing research, that also includes the study of the possible bifurcations of pulses. Such bifurcations may by themselves generate complex, and not yet understood, dynamics – see Fig. 5(c).

5.1.2 N-component models

There is a huge gap between the complexity of scalar equations – i.e. $N = 1$ in (1.1) – and of the 2-component systems (1.2) considered so far, both in the analysis of the models – see sections 4.1.1, 4.2.1 and 4.3.1 – and in the dynamics exhibited by the models. We are not aware of a similar gap between 2-component and $N \geq 3$-component systems. All 'tools' presented in sections 2-4 can be applied to system (1.1) with $N \geq 3$; the generic results of Lemmas 3.1, 4.4 and 4.5 also still hold (with in essence identical proofs). Nevertheless, the analysis of an explicitly given N-component system is considerably more involved than of a 2-component system (which motivated our choice to focus on (1.2)) – see for instance [26, 87, 88] for an existence, stability and front interaction analysis of a 3-component FitzHugh-Nagumo model – Remark 4.13 – along the lines of this text. Moreover, the present mathematical understanding of the dynamics generated by $N \geq 3$-component systems still is relatively limited. For instance, there are reasons to expect that a third component is necessary to stabilize uniformly travelling spots – i.e. localized homoclinic structures in $\mathbb{R}^2$ (section 5.2.2) – see [89] and the references therein.

5.2 Pattern formation in $\mathbb{R}^2$

Although system (1.1) certainly also is relevant in domains of dimension ≥ 3, we focus on patterns in $\mathbb{R}^2$.

5.2.1 At onset

The weakly nonlinear Ginzburg-Landau approach presented in sections 2.2, 2.3, 2.4 and 2.5 has been developed for classes of evolutionary systems *on cylindrical domains* Ω that are much more general than reaction-diffusion system (1.1) – see section 5.3. However, for the non-cylindrical domain $\Omega = \mathbb{R}^2$, the theory is less well-developed. This is due to the fact that the simple reversibility $x \to -x$ symmetry of (1.1) in $\mathbb{R}^1$ now is generalized to the much larger class of 'rigid transformations' of the Euclidian group

$E(2)$. In more explicit terms: in $\mathbb{R}^2$, the linear decomposition (2.1) generalizes to,

$$(U(x,y,t), V(x,,yt)) = (\bar{U}, \bar{V}) + (\alpha, \beta)e^{i(kx+\ell y)+\lambda t}, \tag{5.39}$$

now with $k, \ell \in \mathbb{R}$. This has virtually no 'computational impact' on the subsequent spectral Turing analysis of section 2.1, since one only needs to replace the k^2-terms in (2.2) by $k^2 + l^2$. However, this does imply that the band(s) of unstable wave numbers (2.14) of Lemma 2.1 must be replaced by the 'ring',

$$\sqrt{\frac{dg_u^c + h_v^c}{2d}} - \varepsilon\sqrt{\frac{2\lambda_\mu^c \tilde{\mu}}{|\lambda_{k^2}^c|}} + \mathcal{O}(\varepsilon^2) < \sqrt{k^2+\ell^2} < \sqrt{\frac{dg_u^c + h_v^c}{2d}} + \varepsilon\sqrt{\frac{2\lambda_\mu^c \tilde{\mu}}{|\lambda_{k^2}^c|}} + \mathcal{O}(\varepsilon^2) \tag{5.40}$$

(cf. (2.5), (2.10)). As a consequence, many linearly unstable perturbations *with distinct spatial structures* will grow exponentially. For instance, (vertical) *stripe patterns* correspond to $(k, \ell) = (k_c + \varepsilon\tilde{k}, 0)$ with $\tilde{k}$ as in (2.14), these are the direct 2-dimensional counterparts of 1-dimensional structures of Lemma 2.1 (trivially extended in the y-direction). However, perturbations associated to intersections of the lines $\ell = \pm\sqrt{3}k$ with the ring (5.40) drive the formation of *hexagonal patterns* [37]. The bifurcation of small amplitude stripe and hexagonal patterns can be studied by a *finite dimensional* center manifold reduction [37]; the derivation of the governing equations is similar to that of section 2.2, but with amplitudes that do not depend on ξ, i.e. the end product is not a PDE – like (2.29) – but a system of ODEs [37]. As a consequence, it is not possible to obtain decisive results on the stability of the bifurcating patterns *against general (bounded) perturbations* (since the approximation scheme cannot cover all unstable perturbations described by the ring (5.40)). Although there is a huge literature on this problem – see for instance [13] – there is at present no conclusive mathematical theory on the onset of pattern formation in systems defined on $\mathbb{R}^2$ (and/or $\mathbb{R}^n$ for $n \geq 2$).

5.2.2 Far from equilibrium

As is already clear from Fig. 1, the far from equilibrium dynamics exhibited by reaction-diffusion systems can be overwhelmingly rich and complex. We do not intend to discuss the phenomenology of these dynamics and instead choose to focus on the most simple *localized* far from equilibrium structures.

• **Spots.** An isolated localized spot for system (1.1) defined on $\mathbb{R}^2$ can be seen as a homoclinic solution to the (inhomogeneous) spatial dynamical system associated to stationary, *radially symmetric* solutions of (1.1). For singularly perturbed systems, an existence and stability analysis similar to that of sections 4.2.2 and 4.3.3 can be performed – although the analysis is significantly more involved. Subsequently, an approach to spot interactions can be developed, again in the spirit of – and richer in behavior than – that of pulse interactions in 1 space dimension. See [47, 61, 94, 95] and the references therein.

• **Stripes.** A homoclinic stripe in $\mathbb{R}^2$ is the trivial extension in the y-direction of a 1-dimensional homoclinic pulse (in x). In the singularly perturbed slowly linear setting, these stripes are typically unstable with respect to Turing – sometimes called 'pearling' – instabilities along the stripe [25, 74], unless the fast reduced homoclinic solution of (4.12) is sufficiently close to a heteroclinic cycle [48] (It should be noted though that these claims are based on studies of specific models, at present no general results exist in the literature.) Similar results hold for spatially periodic long wavelength stripes [73].

• **Fronts and interfaces.** Trivially extended 1-dimensional fronts typically are stable. However, these fronts can also be curved or have 'corners'. In the setting of scalar equations there is quite some literature on the description of curvature driven interface dynamics in terms of limiting free boundary value problems. The literature is much more limited for systems, while it is to be expected that these exhibit much more complex interface dynamics. See [11, 40, 56, 81] and the references therein.

5.3 Beyond reaction-diffusion systems

In the final section of his paper [83] on morphogenesis – *pattern formation* – Alan Turing discusses the complex behavior of nonlinear spatial processes, and notes *'One would like to be able to follow this more general process mathematically also. The difficulties are, however, such that one cannot hope to have any very embracing theory of such processes, beyond the statement of the equations.'*. However, these days such an 'embracing theory' does exist *near equilibrium*.

The onset of pattern formation as a parameter μ passes through a critical value μ_c can be studied for large classes of evolutionary systems, including but also *much more general* than the reaction-diffusion systems considered here. If the destabilization is caused by discrete spectrum, we are in the 'standard' setting of bifurcation theory and the dynamics of the full system can be described by center manifold reductions – see [39, 84]. If the essential spectrum is the driving mechanism – and the system is thus defined on an unbounded domain – then a weakly nonlinear approach along the lines of sections 2.2 and 2.5 can be performed. It's crucial however that the spatial domain is *cylindrical*, i.e. of the type $\tilde{\Omega} \times \mathbb{R}$ with $\tilde{\Omega} \in \mathbb{R}^d$ $(d \geq 0)$ bounded – see section 5.2.1. Like in section 2, for μ sufficiently close to μ_c the evolution of small perturbations of a basic state $\overline{\mathbf{U}}$ – measured in a well-chosen norm – can be captured for a *finite, but asymptotically large, time* by a modulation equation – typically the *complex Ginzburg-Landau equation* (cf. (2.43)) – that depends on only one spatial variable (corresponding to the unbounded direction of the cylinder). We refer to [2, 13, 54] and the references therein for further, detailed discussions.

Beyond the 'near equilibrium'-setting, Turing's 'embracing theory' indeed does not exist. Nevertheless, it can be claimed that Alan Turing – *'one cannot hope'* – was overly pessimistic, since also our insights in localized structures and their interactions – as sketched in the preceding sections – have evolved into a more general 'tool' by which fundamental insights in the complexity of spatial processes can be obtained: the basic ideas presented here form the foundation of a much more general approach that has been shown to be relevant and powerful way beyond the reaction-diffusion context.

Acknowledgements. The author likes to thank Robbin Bastiaansen for providing Fig. 1(b) and Fig. 5(a) and Mark Peletier and Mara Smeele for commenting on an earlier version of the manuscript.

References

[1] J. Alexander, R. Gardner & C.K.R.T Jones, A topological invariant arising in the stability analysis of traveling waves, *J. Reine Angew. Math.* **410** (1990) 167-212.

[2] I.S. Aranson & L. Kramer, The world of the complex GinzburgLandau equation, *Rev. Mod. Phys.* **74** (2002) 99-143.

[3] T. Bellsky, A. Doelman, T. J. Kaper & K. Promislow, Adiabatic stability under semi-strong interactions: The weakly damped regime, *Indiana Univ. Math. J.* **62** (2013) 1809-1859.

[4] T.B. Benjamin & J.E. Feir, The disintegration of wave trains on deep water Part 1. Theory, *J. Fluid Mech.* **27**(3) (1967) 417-430.

[5] J. Bitzer & G. Schneider, Approximation and attractivity properties of the degenerated Ginzburg-Landau equation, *J. Math. Anal. Appl.* **331**(2) (2007) 743778.

[6] F.H. Busse, Non-linear properties of thermal convection, *Rep. Prog. Phys.* **41**(12) (1978) 1929-1967.

[7] J. Carr & R.L. Pego, Metastable patterns in solutions of $u_t = \varepsilon^2 u_{xx} - f(u)$, *Comm. Pure Appl. Math.* **42**(5) (1989) 523-576.

[8] P. Carter, B. de Rijk & B. Sandstede, Stability of traveling pulses with oscillatory tails in the FitzHugh-Nagumo system, *J. Nonlinear Sci.* **26**(5) (2016) 1369-1444.

[9] P. Carter & B. Sandstede, Fast pulses with oscillatory tails in the FitzHugh-Nagumo system, *SIAM J. Math. Anal.* **47**(5) (2015) 3393-3441.

[10] W. Chen & M.J. Ward, Oscillatory instabilities and dynamics of multi-spike patterns for the one-dimensional Gray-Scott model, *Europ. J. Appl. Math.* **20**(2) (2009) 187-214.

[11] X. Chen, Generation and propagation of interfaces in reaction-diffusion systems, *Trans. Amer. Math. Soc.* **334**(2) (1992) 877-913.

[12] P. Collet & J.-P. Eckmann, The time dependent amplitude equation for the Swift-Hohenberg problem, *Comm. Math. Phys.* **132**(1) (1990) 139-153.

[13] M.C. Cross & P.C. Hohenberg, Pattern formation outside of equilibrium, *Rev. Mod. Phys.* **65** (1993) 851-1112.

[14] R.C. Diprima, W. Eckhaus & L.A. Segel, Non-linear wave-number interaction in near-critical two-dimensional flows, *J. Fluid Mech.* **49**(4) (1971) 705-744.

[15] B. de Rijk, A. Doelman & J.D.M. Rademacher, Spectra and stability of spatially periodic pulse patterns: Evans function factorization via Riccati transformation, *SIAM J. Math. Anal.* **48**(1) (2016) 61-121.

[16] A. Doelman & W. Eckhaus, Periodic and quasi-periodic solutions of degenerate modulation equations, *Physica D* **53**(2-4) (1991) 249-266.

[17] A. Doelman, R.A. Gardner & T.J. Kaper, Stability analysis of singular patterns in the 1-D Gray-Scott model: A matched asymptotics approach, *Physica D* **122**(1) (1998) 1-36.

[18] A. Doelman, R.A. Gardner, & T.J. Kaper, Large stable pulse solutions in reaction-diffusion equations, *Indiana Univ. Math. J.* **50**(1) (2001) 443-507.

[19] A. Doelman & T. J. Kaper, Semi-strong pulse interactions in a class of coupled reaction-diffusion equations, *SIAM J. Appl. Dyn. Syst.* **2** (2003) 53-96.

[20] A. Doelman, T. J. Kaper & K. Promislow, Nonlinear asymptotic stability of the semi-strong pulse dynamics in a regularized Gierer-Meinhardt model, *SIAM J. Math. Anal.* **38** (2007) 1760-1787.

[21] A. Doelman, T.J. Kaper & H. van der Ploeg, Spatially periodic and aperiodic multi-pulse patterns in the one-dimensional Gierer-Meinhardt equation, *Meth. Appl. Anal.* **8**(2) (2001) 387-414.

[22] A. Doelman, T.J. Kaper & P. Zegeling, Pattern formation in the one-dimensional Gray-Scott model, *Nonlinearity* **10**(2) (1997) 523-563.

[23] A. Doelman, J.D.M. Rademacher, B. de Rijk & F. Veerman, Destabilization mechanisms of periodic pulse patterns near a homoclinic limit, to appear in *SIAM J. Appl. Dyn. Syst.* (2018).

[24] A. Doelman, J.D.M. Rademacher & S. van der Stelt, Hopf dances near the tips of Busse balloons, *Discrete Contin. Dyn. Syst. Ser. S* **5**(1) (2012) 61-92.

[25] A. Doelman & H. van der Ploeg, Homoclinic stripe patterns, *SIAM J. Appl. Dyn. Syst.* **1**(1) (2002) 65104.

[26] A. Doelman, P.J.A. van Heijster & T.J. Kaper, Pulse dynamics in a three-component system: existence analysis, *J. Dynam. Differential Equations* **21**(1) (2009) 73115.

[27] A. Doelman, P.J.A. van Heijster & F. Xie, A geometric approach to stationary defect solutions in one space dimension, *SIAM J. Appl. Dyn. Syst.* **15**(2) (2016) 655-712.

[28] A. Doelman & F. Veerman, An explicit theory for pulses in two component, singularly perturbed, reaction-diffusion equations, *J. Dynam. Differential Equations* **27**(3-4) (2015) 555-595.

[29] W. Eckhaus, *Studies in non-linear stability theory*, *Springer Tracts in Natural Philosophy* **6** (1965), Springer.

[30] W. Eckhaus, The Ginzburg-Landau manifold is an attractor, *J. Nonlinear Sci.* **3**(3) (1993) 329-348.

[31] S.-I. Ei, The motion of weakly interacting pulses in reaction-diffusion systems, *J. Dynam. Differential Equations* **14** (2002) 85-137.

[32] N. Fenichel, Geometrical singular perturbation theory for ordinary differential equations, *J. Differential Equations* **31** (1979) 53-98.

[33] B. Fiedler & A. Scheel, Spatio-temporal dynamics of reaction-diffusion patterns, pp 23-152 in M. Kirkilionis, S. Krömker, R. Rannacher, F. Tomi (eds) *Trends in Nonlinear Analysis* (2003) Springer.

[34] G. Fusco & J.K Hale, Slow-motion manifolds, dormant instability, and singular perturbations, *J. Dynam. Differential Equations* **1**(1) (1989) 75-94.

[35] R.A. Gardner, On the structure of the spectra of periodic travelling waves, *J. Math. Pures Appl.* (9) **72** (1993) 415-439.

[36] A. Gierer & H. Meinhardt, A theory of biological pattern formation, *Kybernetik* **12**(1) (1972) 30-39.

[37] M. Golubitsky, I. Stewart & D.G. Schaeffer, *Singularities and groups in bifurcation theory II*, Applied Mathematical Sciences **69** (1988) Springer.

[38] K. Gowda, H. Riecke & M. Silber, Transitions between patterned states in vegetation models for semiarid ecosystems, *Phys. Rev. E* **89** (2014) 022701.

[39] M. Haragus & G. Iooss, *Local bifurcations, center manifolds, and normal forms in infinite-dimensional dynamical systems*, Universitext, (2011) Springer.

[40] M. Haragus, A. Scheel, Corner defects in almost planar interface propagation, *Ann. Inst. H. Poincaré Anal. Non Linéaire* **23**(3) (2006) 283-329.

[41] D. Henry, *Geometric Theory of Semilinear Parabolic Equations*, Lecture Notes in Mathematics **840** (1981) Springer.

[42] C.K.R.T. Jones, Stability of the travelling wave solution of the FitzHugh-Nagumo system, *Trans. Amer. Math. Soc.* **286**(2) (1984) 431-469.

[43] C.K.R.T. Jones, Geometric singular perturbation theory, in *Dynamical systems, Montecatibi Terme, 1994*, Lecture Notes in Mathematics **1609**, R. Johnson (ed.), Springer (1995).

[44] T. Kapitula, On the nonlinear stability of plane waves for the Ginzburg-Landau equation, *Comm. Pure Appl. Math.* **47**(6) (1994) 831841.

[45] T. Kapitula & K. Promislow, *Spectral and dynamical stability of nonlinear waves*, Applied Mathematical Sciences **185** (2013) Springer.

[46] J. Keener & J. Sneyd, *Mathematical Physiology*, Interdisciplinary Applied Mathematics **8** (1998) Springer.

[47] T. Kolokolnikov, M.J. Ward & J. Wei, Spot self-replication and dynamics for the Schnakenburg model in a two-dimensional domain, *J. Nonlinear Sci.* **19**(1) (2009) 1-56.

[48] T. Kolokolnikov, M. Ward, W. Sun & J. Wei, The stability of a stripe for the Gierer-Meinhardt model and the effect of saturation, *SIAM J. Appl. Dyn. Systems* **5**(2) (2006) 313-363.

[49] Y. Kuramoto, *Chemical oscillations, waves, and turbulence*, Springer Series in Synergetics **19** (1984) Springer.

[50] Y. Kuramoto & T. Tsuzuki, Reductive Perturbation Approach to Chemical Instabilities, *Progr. Theor. Physics* **52**(4) (1974) 1399-1401.

[51] K.-J. Lin, W.D. McCormick, J.E. Pearson & H.L. Swinney, Experimental observation of self-replicating spots in a reaction-diffusion system, *Nature* **369** (1994) 215-218.

[52] B.J. Matkowsky & V.A. Volpert, Stability of plane wave solutions of complex Ginzburg-Landau equations, *Quart. Appl. Math.* **51** (1993) 265-281.

[53] E. Meron, *Nonlinear Physics of Ecosystems* (2015) CRC Press.

[54] A. Mielke, The Ginzburg-Landau equation in its role as a modulation equation, in *Handbook of Dynamical Systems* **2**, North-Holland, Amsterdam (2002) 759-834.

[55] D.S. Morgan, A. Doelman & T.J. Kaper, Stationary periodic patterns in the 1D Gray-Scott model, *Meth. Appl. Anal.* **7**(1) (2000) 105-149.

[56] L. Mugnai & R. Matthias, Convergence of perturbed Allen-Cahn equations to forced mean curvature flow, *Indiana Univ. Math. J.* **60**(1) (2011) 41-75.

[57] J.D. Murray, *Mathematical Biology*, *Biomathematics* **19** (1989) Springer.

[58] A.C. Newell, Envelope equations, *Lect. Appl. Math.* **15** (1974) 157163.

[59] A.C. Newell & J.A. Whitehead, Finite bandwidth, finite amplitude convection, *J. Fluid Mech.* **38**(2) (1969) 279-303.

[60] W.-M. Ni, Diffusion, cross-diffusion, and their spike-layer steady states, *Notices AMS* **45** (1998) 9-18.

[61] W.-N. Ni & J. Wei, On positive solutions concentrating on spheres for the Gierer-Meinhardt system, *J. Differential Equations* **221**(1) (2006) 158-189.

[62] Y. Nishiura & D. Ueyama, Spatio-temporal chaos for the GrayScott model, *Phyica D* **150**(3) (2001) 137-162.

[63] J.E. Pearson, Complex patterns in a simple system, *Science* **261** (1993) 189-192.

[64] K. Promislow, A renormalization method for modulational stability of quasi-steady patterns in dispersive systems, *SIAM J. Math. Anal.* **33** (2002) 1455-1482.

[65] J.D.M. Rademacher & A. Scheel, Instabilities of wave trains and Turing patterns in large domains, *Internat. J. Bifur. Chaos Appl. Sci. Engrg.* **17**(8) (2007) 2679-2691.

[66] J.D.M. Rademacher, B. Sandstede & A. Scheel, Computing absolute and essential spectra using continuation, *Physica D* **229**(2) (2007) 166-183.

[67] W.N. Reynolds, J.E Pearson & S. Ponce-Dawson, Dynamics of self-replicating patterns in reaction diffusion systems, *Phys. Rev. Lett.* **72** (1994) 2797-800.

[68] M.G. Rietkerk & J. van de Koppel, Regular pattern formation in real ecosystems, *Trends in Ecology & Evolution* **23**(3) (2008) 169-175.

[69] V. Rottschäfer & A. Doelman, On the transition from the Ginzburg-Landau equation to the extended Fisher-Kolmogorov equation, *Physica D* **118**(3-4) (1998) 261-292.

[70] B. Sandstede, Stability of Travelling Waves, in *Handbook of Dynamical Systems* **2**, North-Holland (2002) 983-1055.

[71] G. Schneider, Hopf bifurcation in spatially extended reaction-diffusion systems, *J. Nonlinear Sci.* **8**(1) (1998) 17-41.

[72] G. Schneider, Nonlinear diffusive stability of spatially periodic solutions – abstract theorem and higher space dimensions, *Tohoku Math. Publ.* **8** (1998) 159-167.

[73] L. Sewalt & A. Doelman, Spatially periodic multi-pulse patterns in a generalized KlausmeierGrayScott model, *SIAM J. Appl. Dyn. Syst.* **16**(2) (2017) 1113-1163.

[74] E. Siero, A. Doelman, M.B. Eppinga, J.D.M. Rademacher, M. Rietkerk & K. Siteur, Striped pattern selection by advective reaction-diffusion systems: resilience of banded vegetation on slopes, *Chaos* **25**(3) (2015) 036411.

[75] A. Shepeleva, On the validity of the degenerate Ginzburg-Landau equation, *Math. Methods Appl. Sci.* **20**(14) (1997) 1239-1256.

[76] J.A. Sherratt, History-dependent patterns of whole ecosystems, *Ecological Complexity* **14** (2013) 8-20.

[77] K. Siteur, E. Siero, M.B. Eppinga, J.D.M. Rademacher, A. Doelman & M. Rietkerk, Beyond Turing: The response of patterned ecosystems to environmental change, *Ecological Complexity* **20** (2014) 81-96.

[78] J. Smoller, *Shock waves and reaction-diffusion equations*, *Grundlehren der Mathematischen Wissenschaften* **258** (1983), Springer.

[79] K. Stewartson & J.T. Stuart, A non-linear instability theory for a wave system in plane Poiseuille flow, *J. Fluid Mech.* **48**(3) (1971) 529-545.

[80] J.T. Stuart & R.C. DiPrima, The Eckhaus and Benjamin-Feir resonance mechanims, *Proc. Roy. Soc. A* **362**(1708) (1978) 27-41.

[81] M. Taniguchi & Y. Nishiura, Instability of planar interfaces in reaction-diffusion systems, *SIAM J. Math. Anal.* **25**(1) (1994) 99134.

[82] R. Temam, *Infinite-dimensional dynamical systems in mechanics and physics* (2nd ed.), Applied Mathematical Sciences **68** (1997), Springer.

[83] A. M. Turing, The chemical basis of morphogenesis, *Phil. Trans. Roy. Soc. London B* **237** (1952) 37-72.

[84] A. Vanderbauwhede & G. Iooss, Centre manifold theory in infinite dimensions, *Dynamics Reported* **1** (1992) 125-163.

[85] S. van der Stelt, A. Doelman, G.M. Hek & J.D.M. Rademacher, Rise and fall of periodic patterns for a generalized Klausmeier-Gray-Scott model, *J. Nonlinear Sci.* **23**(1) (2013) 39-95.

[86] A. van Harten, On the validity of the Ginzburg-Landau equation, *J. Nonlinear Sci.* **1**(4) (1991) 397-422.

[87] P.J.A. van Heijster, A. Doelman & T.J. Kaper, Pulse dynamics in a three-component system: stability and bifurcations, *Physica D* **237**(24) (2008) 3335-3368.

[88] P.J.A. van Heijster, A. Doelman, T. J. Kaper & K. Promislow, Front interactions in a three-component system, *SIAM J. Appl. Dyn. Syst.* **9**(2) (2010) 292-332.

[89] P.J.A. van Heijster & B. Sandstede, Bifurcations to travelling planar spots in a three-component FitzHugh-Nagumo system, *Physica D* **275** (2014) 19-34.

[90] F. Veerman, Breathing pulses in singularly perturbed reaction-diffusion systems, *Nonlinearity* **28**(7) (2015) 2211-2246.

[91] F. Veerman & A. Doelman, Pulses in a Gierer-Meinhardt equation with a slow nonlinearity, *SIAM J. Appl. Dyn. Syst.* **12**(1) (2013) 28-60.

[92] A.I. Volpert, V.A. Volpert & V.A. Volpert, *Traveling Wave Solutions of Parabolic Systems*, Translations Math. Monographs **140** (1994) AMS.

[93] M.J. Ward & J. Wei, Hopf bifurcations and oscillatory instabilities of spike solutions for the one-dimensional Gierer-Meinhardt model, *J. Nonlinear Sci.* **13**(2) (2003) 209-264.

[94] J. Wei & M. Winter, On the two-dimensional Gierer-Meinhardt system with strong coupling, *SIAM J. Math. Anal.* **30**(6) (1999) 1241-1263.

[95] J. Wei & M. Winter, *Mathematical aspects of pattern formation in biological systems*, Applied Mathematical Sciences **189** (2014) Springer.

[96] S. Zelik & A. Mielke, Multi-pulse evolution and space-time chaos in dissipative systems, *Mem. Amer. Math. Soc.* **198**(925) (2009).

[97] Y.R. Zelnik, E. Meron & G. Bel, Gradual regime shifts in fairy circles, *Proc. Natl. Acad. Sci. USA* **112**(40) (2015) 12327-12331.